3

The Production of Colour by Reflection

- **Why are soap bubbles coloured?**
- **How do antireflection coatings on lenses function?**
- **How can perfect mirrors be made from transparent materials?**

Reflection is a commonplace phenomenon and the appearance of a solid is often dominated by reflection. As well as modifying the perceived colour of a body in terms of surface gloss, reflection as such can give rise to a surprising range of colours. The most vivid of these are associated with the presence of reflection by thin transparent films. Bright colours are often seen in soap bubbles, and close examination of transparent insect wings shows that these can show areas which are beautifully coloured. Casual observation also reveals that the colours have a metallic aspect (due to a considerable specular component) and seem to vary with the direction of viewing and with the thickness of the film. They are said to be *iridescent*. In this chapter the origin of these and other colours due to reflection is explored. Attention is confined to reflection by more or less transparent insulating solids (dielectrics in older literature). Metals are considered in a later chapter. However, recall that the refractive index varies with wavelength, and metals are transparent at some wavelengths and in these circumstances the conclusions of this chapter will then apply.

It is necessary to mention that polarisation of light is important in reflection. In this chapter we are concerned mainly with the colours produced by unpolarised sunlight, and the refinements needed to account for the polarisation of the waves are considered in Chapter 4. This objective is aided by mainly considering light falling perpendicularly onto surfaces, for which the polarisation direction of the wave becomes redundant.

Colour and the Optical Properties of Materials: An Exploration of the Relationship Between Light, the Optical Properties of Materials and Colour, Second Edition
Richard J. D. Tilley
 ISBN: 978-0-470-74696-7

3.1 Reflection from a Single Surface

3.1.1 Reflection from a transparent plate

When light falls onto a *smooth*, thick transparent plate such as a slab of glass, so that the lower surface can be ignored, some of it will be reflected and some transmitted (Figure 3.1). For a smooth metal plate almost all of the light will be reflected, as the amount of transmitted light is negligible. For both materials, the well-known law of reflection is:

$$\theta_1 = \theta_3$$

where θ_1 (also θ_i or i) is the *angle of incidence* and θ_3 (also θ_r or r) the *angle of reflection*. The *plane of incidence* contains the incident ray, the reflected ray and the normal to the reflecting surface. In Figure 3.1 this is the plane of the page.

The amount of light reflected from such a surface depends upon the polarisation of the light (Chapter 4). For a polished, thick plate and light at *normal incidence* (i.e. perpendicular to the surface) the polarisation can be ignored and the *coefficient of reflection* r, defined such that if a wave of *amplitude* $\mathcal{E}_0$ falls upon the surface then the *amplitude* of the reflected wave is $r\mathcal{E}_0$, is given by:

$$r = \frac{n_0 - n_s}{n_0 + n_s}$$

where n_0 and n_s are the refractive indices of the media on the two sides of the boundary in the direction in which the light travels (Figure 3.2). The eye detects *irradiance* changes rather than amplitude changes, and so it is the more convenient to work with the *reflectivity* or *reflectance* R:

$$R = r^2 = \left(\frac{n_0 - n_s}{n_0 + n_s}\right)^2$$

This is because the irradiance I_0 is proportional to the square of the amplitude $\mathcal{E}_0^2$. The reflected irradiance $R(I_0)$ (Figure 3.2) is then proportional to $r^2\mathcal{E}_0^2$.

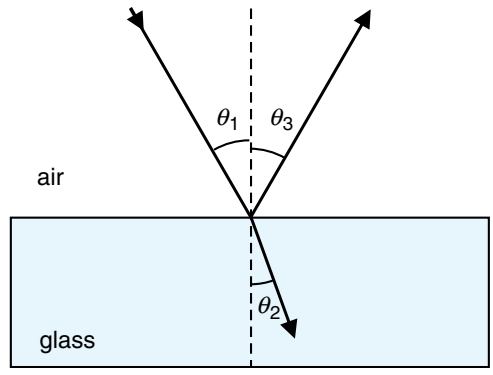

Figure 3.1 ***Light falling on a transparent plate such as a slab of glass will be partly reflected and partly refracted. The angle of incidence θ_1 will be equal to the angle of reflection θ_3***

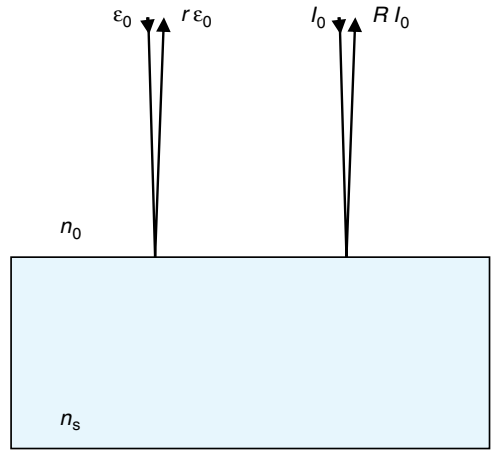

Figure 3.2 ***Reflection of a beam of light perpendicular to a transparent surface. The amplitude of the incident beam is $\mathcal{E}_0$ and incident irradiance is I_0. The reflected amplitude will be given by $r\mathcal{E}_0$ and the reflected intensity by RI_0. The angles have been exaggerated for clarity***

Remember that because n depends upon wavelength, the coefficient of reflection and the reflectivity will vary across the spectrum.

When light travelling through a medium of low refractive index (such as air) is reflected at the surface of a substance of higher refractive index (such as glass), r is negative. This signifies a phase change of π radians on reflection, which means, in terms of a light wave, that a peak turns into a trough, and vice versa, whenever the refractive indices at the interface are in the sequence low/high (Figure 3.3).

The reflectivity R for a transparent plate of refractive index n_s in air is:

$$R = \left(\frac{1-n_s}{1+n_s}\right)^2 = \left(\frac{n_s-1}{n_s+1}\right)^2 \tag{3.1}$$

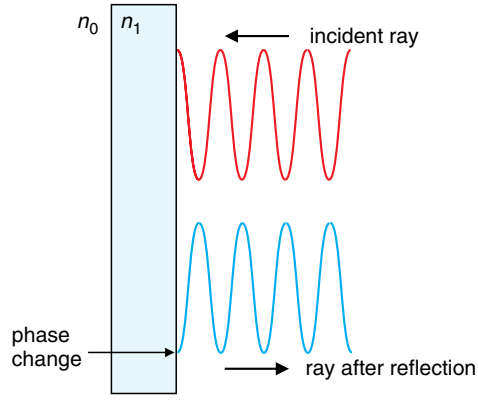

Figure 3.3 ***A phase change of π radians is introduced in a ray reflected at a surface of higher refractive index, which means that a peak changes to a trough and vice versa***

For ordinary glass, with a refractive index of approximately 1.5, R is about 0.03–0.04; that is, about 3–4 %. Although this may seem to be a rather insignificant amount, it is noticeable in everyday life. Reflections from windows and from the glass over a painting are frequently annoying. Moreover, it is too high for specialist purposes, such as high-performance lenses and optical components, so these are given antireflection coatings, discussed below. In addition, this small degree of reflectivity turns out to be an essential component in the production of colour through interference by thin films.

3.1.2 Data storage using reflection

In essence, the active data storage layer (or layers) on CDs, DVDs, HD-DVDs and Blu-Ray discs is reflective. Data is stored by making small dots on the recording layer that have a different reflectivity to the background. The writing process involves decreasing the reflectivity and the reading process involves detecting these reflectivity differences.

The discs that contain permanent read-only data, such as those sold in stores, are produced with physical pits in the surface. The pit will have a different reflectivity to the higher surrounding plateau. The smaller the pit, the more data can be stored on the disc. Pit size is more or less controlled by the wavelength of the light used to record the data. The CD, introduced in 1983, used infrared wavelengths (780 nm) generated by semiconductor lasers (Section 10.9). The pit size minimum was 0.83 μm and the track pitch (the separation between lines of pits) was 1.6 μm. Great effort was expended in moving towards red light, wavelength 650 nm, which allowed for smaller pit dimensions. Thus, the DVD, introduced in 1996, using this wavelength, has a minimum pit size of 0.4 μm and a track pitch of 0.74 μm. Recently, there has been a move to blue light, wavelength 405 nm, allowing for smaller pits and greater data storage, resulting in the transition to HD-DVD and Blu-ray technology.

Recordable CDs (CD-R) use similar reflectivity differentials to record data. In this instance, a writing laser in the computer marks small spots in a layer of polymer containing a dye. These spots are detected as changes in reflectivity when scanned by the reading laser. Rewritable CDs (CD-RW) make marks in a layer of a crystalline Ag–In–Sb–Te alloy. The exact composition of the alloy is carefully chosen so as to yield optimum recording and erasing facilities under the influence of the lasers normally present in home computers. The alloy is crystalline as prepared. When heated by a pulse from the writing laser beam, to a temperature of approximately 700 °C, the alloy melts locally and cools too rapidly to crystallise, thus ending in an amorphous (glass-like) state. This has a lower reflectivity than the surrounding crystalline surface. Erasure is carried out by heating the amorphous data spot with a laser pulse to about 200 °C, which allows solid-state crystallisation to occur, restoring the original surface reflectivity. The writing process can then be carried out once more.

The marks on a CD or DVD are comparable in size to the wavelength of light. This means that light rays can interfere and produce iridescent colours. These are discussed in terms of diffraction in Chapter 6.

3.2 Interference at a Single Thin Film in Air

Part of a monochromatic beam of light incident upon the top surface of a homogeneous thin film of refractive index n will be reflected. The remainder will enter the film and be repeatedly reflected from the bottom surface and the underside of the top surface. At each reflection some of the light will escape to produce additional reflected and transmitted rays (Figure 3.4a). The consequence of this repeated reflection and transmission is to produce the bright colours seen on thin films of many types.

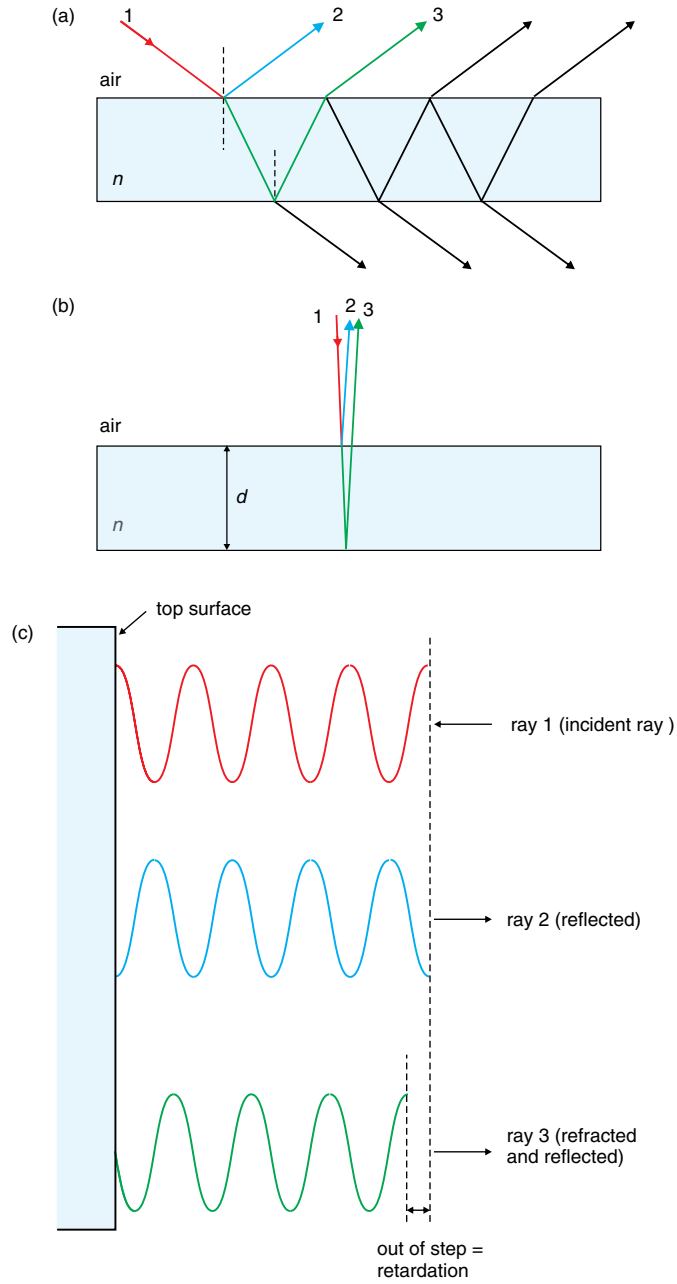

Figure 3.4 ***The reflection and transmission of a ray of light incident on a transparent film in air. (a) A number of reflected and transmitted beams occur due to repeated reflection at the top and bottom faces of the film. (b) At normal incidence (the angles of incidence and reflection have been changed from 90° for clarity), ray 3 will have travelled further than ray 2 by a path difference of 2nd. (c) The waves making up rays 2 and 3 will be out of step due to the combined effects of a phase change on reflection and the path difference***

3.2.1 Reflection perpendicular to the film

When the light beam is perpendicular to the surface the complexity of dealing with polarisation is avoided, so that the analysis of the phenomenon is simplified. In this case, part of the light seen by an observer above the film will have been reflected at the top surface (ray 2). In addition, some will have travelled through the film and been reflected from the bottom surface before reaching the observer (ray 3) (Figure 3.4b). As the reflectivity is rather small, about 4 % for a glass surface, the first reflected ray and the first ray transmitted through the glass and then reflected from the lower surface are of most importance. For the present, the other transmitted and reflected rays will be ignored.

Because of the difference in the paths taken by the two rays, the waves will be out of step. In addition, because ray 2 is travelling through a medium of low refractive index and is reflected at a low–high refractive index interface a wave peak will turn into a trough and vice versa. This will not happen to ray 3 because it is reflected at a high–low refractive index surface (Figure 3.4c).

On leaving the thin film the waves making up rays 2 and 3 can now interfere, which will cause the film to look either dark or bright. The effect is easily understood. Ray 3 will have travelled further than ray 2 by a twice the film thickness, $2d$. However, the physical thickness does not give the mismatch between the wave crests and peaks of these two rays. This is given by the additional optical path travelled by ray 3, in this case $2nd$, where n is the refractive index of the film and d is the physical thickness. The *path difference* (or *retardation*) between rays 2 and 3 is equal to the optical path difference between the two rays, so that:

$$p = 2nd$$

The appearance of a thin film when viewed by reflection at normal incidence will depend upon this path difference. If the path difference p considered in isolation is equal to an integral number of wavelengths then the waves will be exactly in step as they travel away from the surface. Adding in the phase change of half a wavelength for ray 2 will make it out of step with ray 3 by this amount as they leave the surface. The consequence is that destructive interference will occur between ray 2 and ray 3. The film will, therefore, appear dark. In general, the film will appear dark under irradiation with light of wavelength λ_0 in air when:

$$p = 2nd = m\lambda_0 \quad (m = 1, 2, 3, \ldots) \qquad \textbf{minimum} \text{ (dark)}$$

In a similar way, a path difference p between ray 2 and ray 3 equal to a half-integral number of wavelengths will cause the two rays to be exactly out of step. Adding in the half-wavelength phase change for ray 2 will make them exactly in step. The film will then appear bright, because constructive interference will occur. In general, the film will appear bright when:

$$p = 2nd = (m + \tfrac{1}{2})\lambda_0 \quad (m = 1, 2, 3, \ldots) \qquad \textbf{maximum} \text{ (bright)}$$

At other path differences the film will appear to have an intermediate tone, depending upon the exact phase difference between ray 2 and ray 3.

When a tapered or wedge-shaped film is viewed by monochromatic light at normal incidence, some thicknesses will be appropriate for constructive interference and some for destructive interference. The film will then appear to be crossed by a series of bright and dark bands (Figure 3.5a and b). When the thickness of the film is considerably below $\frac{1}{2}\lambda_0$ the film will appear dark, because the path difference in the film, $p = 2nd$, will not be sufficient to counteract the change of phase of the ray reflected from the upper surface, and destructive interference occurs. As the film thickness increases, it will eventually reach the stage where the destructive

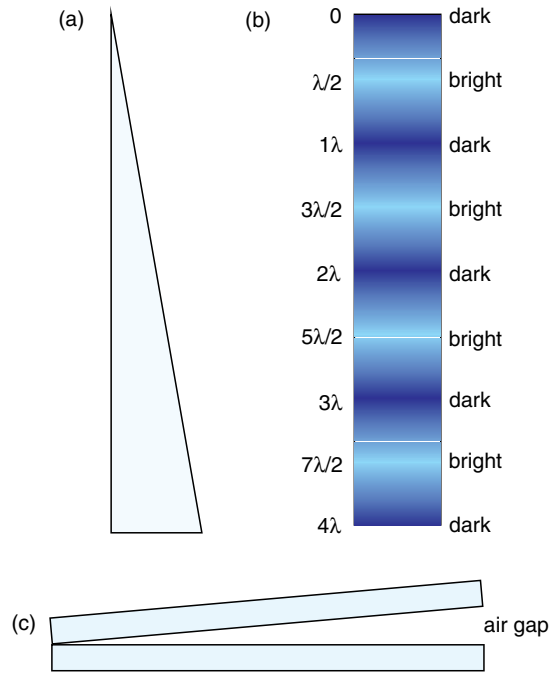

Figure 3.5 ***Interference in a wedge shaped film: (a) film profile; (b) bright and dark reflection bands resulting from the interference of monochromatic light viewed normal to the wedge from above; (c) an air gap between two transparent plates behaves in a similar way to a wedge***

interference is replaced by constructive interference, and a bright band appears, centred at $p = \frac{1}{2}\lambda_0$. Thereafter, bright and dark bands will succeed each other, each at an interval of $p = \frac{1}{2}\lambda_0$.

Precisely the same effect will be obtained for an air wedge between two inclined transparent plates (Figure 3.5c). Bright fringes will be observed as at intervals of:

$$p = 2nd = (m + \tfrac{1}{2})\lambda_0 \quad (m = 1, 2, 3, \ldots) \qquad \textbf{maximum} \text{ (bright)}$$

In cases where the wedge or air gap is not uniform, the fringes follow contours of equal thickness. This gives a dynamic impression of surface contours.

3.2.2 Variation with viewing angle

When the light beam is at an angle to the surface, polarisation effects become important. These are not severe for angles of incidence of up to approximately 25° to the surface (see Figure 4.4) and will be ignored here. The path difference p between rays 2 and 3 becomes (Figure 3.6):

$$p = 2nd\cos\theta_2$$

The analysis now follows that given in the previous section. If p is equal to a whole number of wavelengths then the film will appear dark, due to the combined effect of path difference and change of phase of ray 2 on reflection at the surface. Thus:

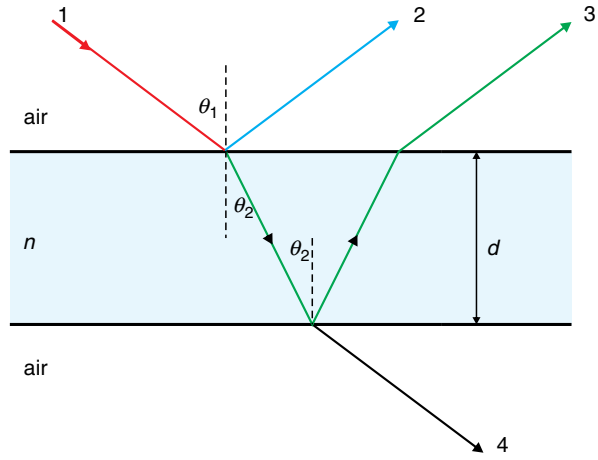

Figure 3.6 ***The reflection of a ray of light incident on a transparent film in air. The path difference between rays 2 and 3 is 2nd cosθ_2***

$$p = 2nd\cos\theta_2 = m\lambda_0 \qquad \textbf{minimum}\ (\text{dark})$$

For the same reason, if the path difference turns out to be a half wavelength, reinforcement will occur and we find:

$$p = 2nd\cos\theta_2 = (m+\tfrac{1}{2})\lambda_0 \qquad \textbf{maximum}\ (\text{bright})$$

When viewed in monochromatic light, the regions of the film which look bright or dark will change with the viewing angle. If the light is normal to the film, then $\cos\theta_2 = \cos(0) = 1$ and the equations reduce to those given in the previous section. Naturally, the same is true of wedges and wedge-shaped air gaps.

3.2.3 Transmitted beams

The analysis given in the preceding section for interference between the reflected beams can be repeated for the transmitted beams (Figure 3.7). The path difference between beams 4 and 5 is:

$$p = 2nd\cos\theta_2$$

In this case, there is no extra phase change, as all reflections take place at the high–low refractive index interfaces. Thus, when:

$$p = 2nd\cos\theta_2 = m\lambda_0 \qquad \textbf{maximum}\ (\text{bright})$$

there will be constructive interference and a maximum in transmitted intensity. When:

$$p = 2nd\cos\theta_2 = (m+\tfrac{1}{2})\lambda_0 \qquad \textbf{minimum}\ (\text{dark})$$

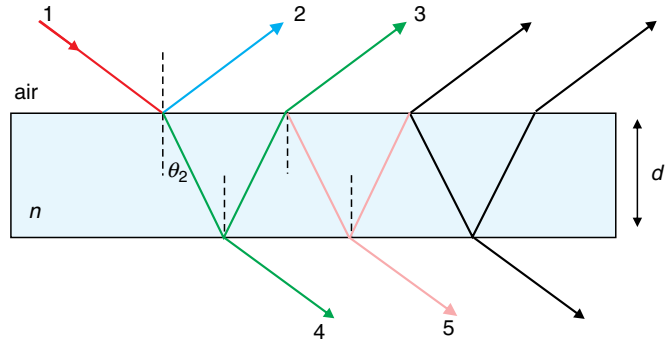

Figure 3.7 ***The transmission of a ray of light incident on a transparent film in air. The path difference between rays 4 and 5 is 2nd cosθ_2***

there will be destructive interference and a minimum in the transmitted intensity. This is converse to the case of reflection, so that a dark reflection band corresponds to a bright transmission band. The two patterns are complementary.

Note, however, the appearances of the patterns are somewhat different. In the case of reflection, the intensities of rays 2 and 3 are similar. In the case of transmission, ray 4 will have approximately 96 % of the incident intensity, while ray 5, which has suffered two reflections, will have about 1/1000 of this value.

3.3 The Colour of a Single Thin Film in Air

Although a discussion of monochromatic light is helpful so as to understand the physical processes taking place on reflection at a thin film, we are really much more interested in what the appearance of the film will be in daylight. When the film is viewed in white light, the same reflection and interference discussed above will occur, except that the effects of all of the different wavelengths present must be added. These interference effects lead to intense colours, familiar in soap films, oil films on water puddles and thin flakes of minerals which can glint with bright colours in sunlight (Figure 3.8).

For example, violet light with a wavelength of 400 nm will reflect a *maximum* of intensity when the film produces a path length difference or retardation $p\ (=2nd)$ of $(m + \frac{1}{2})\lambda$, i.e. 200 nm, 600 nm, 1000 nm and so on (Figure 3.9). Of course, these values of the path difference will not give a maximum for the other wavelengths present in white light. In fact, for a wavelength of 600 nm, there will be a *minimum* of intensity for the same retardation of 600 nm (Figure 3.9).

In order to determine the reflected colour of a thin film when viewed in white light it is necessary to add up all of these contributions over all of the values of the wavelength present. It is seen that there is a large contribution from the 400 nm wave. The contribution from succeeding waves decreases until at a wavelength of 600 nm there is no contribution at all. Thereafter, a small contribution is obtained from wavelengths of 650 and 700 nm. (In reality, a continuum of wavelengths occurs between 400 and 700 nm of course. Here, just seven wavelengths are used as an illustration.) The overall colour perceived will be the sum of all of these. Because of the dominance of the 400 nm contribution the film will appear to be a violet–blue colour. Thereafter, the perceived colour will vary as the film thickness increases or decreases, as certain colours are either reinforced or cancelled. The sequence of colours seen will repeat in a cyclical fashion as the film thickness changes (Figure 3.10). Each sequence of spectral colours is called an *order*, which starts with the *first order* for the

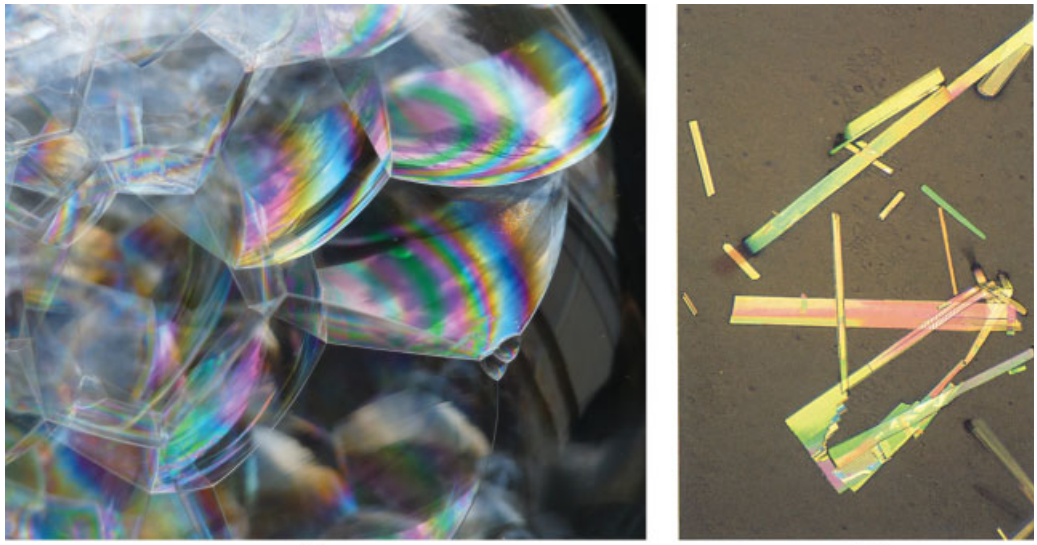

Figure 3.8 ***Interference colours in thin films: (a) soap bubbles; (b) flakes of molybdite (molybdenum trioxide, MoO_3). Both films are viewed in reflected white light***

thinnest of films. A new order begins every 550 nm of retardation (=2*nd*). The colour of a thin film viewed by reflection in white light is given in Appendix A3.1.

Ultimately, strong interference effects will be lost. This is because ordinary white light is emitted in bursts which undergo a sudden change of phase every 10^{-8} s or so. When the film is very thin the two rays which interfere come from within the same burst and interference effects are noticeable. With thicker films, interference takes place between different bursts of light and the interference effects are weaker. This results in films showing mainly pale pinks and greens in the fourth and fifth orders. With even thicker films all interference effects are smoothed out and colours are no longer apparent to the eye.

Since the fraction of incident white light which is reflected is coloured, it follows that the transmitted light will be depleted in this colour and the colour seen will, therefore, be the additive *complementary colour* to that strongly reflected. These are listed in Appendix A3.1.

If the angle of viewing is not perpendicular to the film then the retardation changes slightly. The correct expression for this is:

$$p = 2nd\cos\theta_2$$

as described before. This formula indicates that, as the viewing angle moves away from perpendicular to the film, the colour observed will move towards lower retardation. Thus, for example, second-order orange–red will change towards green and blue (Figure 3.10). (But note that, at all angles except for perpendicular viewing, polarisation will also occur and be important.)

This discussion explains the familiar colours of soap films seen in air. These are best seen if the film is viewed against a black background, which prevents the effects being masked by other reflections. As the thickness of the films varies, due to water flow within the films themselves, the colours change in a dramatic and beautiful way. A draining film has a number of possible equilibrium thicknesses. The thinnest, with a thickness of about 6 nm, gives a black film called Newton's black film. The ways in which a thinning film produces rivers and streams of black in a coloured surrounding film are legion, and no two casually produced films seem to drain in

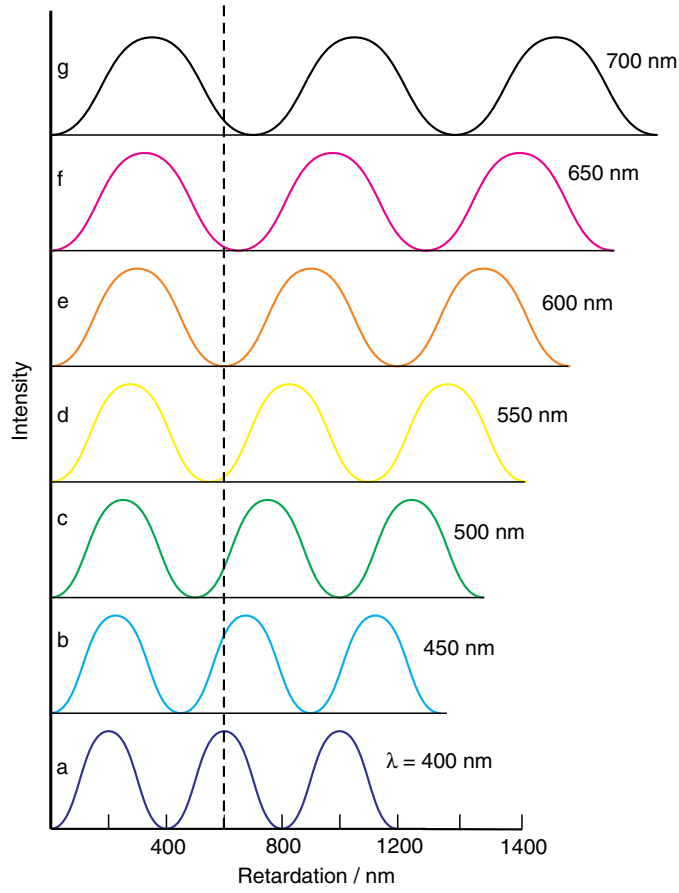

Figure 3.9 ***The intensity (in arbitrary units) of light reflected from a single thin film in air at various wavelengths plotted as a function of the retardation – the optical path difference between the two interfering beams***

the same way. If the films are formed on a wire frame, then the transmitted and reflected colours can be compared.

3.4 The Reflectivity of a Single Thin Film in Air

Interference and colour, as just discussed, should be differentiated from reflectivity. It could be that a certain colour, say red, is produced by interference effects in a film, but whether the colour is readily seen will depend upon the reflectivity of the film for this wavelength. The reflectivity of a thin film in air will be different from that for a thick plate (Equation 3.1), as interference effects from the bottom surface also need to be considered. However, the polarisation of the light will be important and can only be neglected when the light is incident perpendicularly to the surface of the film.

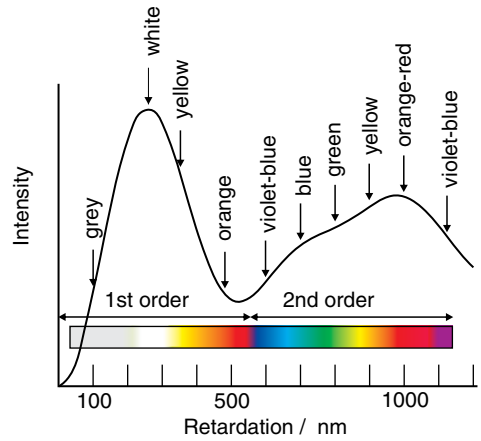

Figure 3.10 ***The total intensity (in arbitrary units) reflected from a thin film in air illuminated by white light as a function of the retardation (the optical path difference) of the film. The approximate colours observed by eye are indicated***

For light of a single wavelength at normal incidence the reflectivity of a homogeneous transparent thin film is given by:

$$R = \frac{2r_1^2 - 2r_1^2\cos 2\delta}{1 - 2r_1^2\cos 2\delta + r_1^4}$$

where

$$r_1 = \frac{n_0 - n_f}{n_0 + n_f}$$

n_0 is the refractive index of the surrounding medium (often air, with $n_0 = 1.0$) and n_f is the refractive index of the film:

$$\delta = \frac{2\pi[d]}{\lambda} = \frac{2\pi n_f d}{\lambda}$$

where $[d]$ is the optical thickness of the film and d is the physical thickness. The reflectivity is found to vary in a cyclic fashion from zero for values of $[d]$ equal to 0, $\lambda/2$, λ, etc. to a maximum (of approximately 0.24 for $n_f = 1.7$) for values of $[d]$ given by $\lambda/4$, $3\lambda/4$ and so on. Because the refractive index of the film is a function of wavelength, the reflectivity will also vary across the spectrum.

3.5 The Colour of a Single Thin Film on a Substrate

The behaviour of a single thin film on a substrate is similar to that discussed for the case of a single thin film in air. Thus, a thin transparent film on a substrate would be coloured when viewed in white light. To analyse this situation, it is necessary to take into account any change of phase that might occur on reflection at the back surface of the film. The actual hue perceived will be found by a summation of all of the reflected intensities, as was discussed earlier.

If the substrate has a *lower refractive index* than the film on the surface then the treatment will be identical to that for a thin film in air, from the point of view of interference effects. The reflected colours observed when the film is viewed at normal incidence in white light will be the same as those listed as 'colour reflected' in Appendix A3.1. (The transmitted colours are normally absorbed by the substrate.)

If the refractive index of the substrate is greater than that of the film then a phase change will be introduced at both the air–film interface and the film–substrate interface. In this case the reflected colour seen at normal incidence when viewed in white light will be the *complementary* colour to that just described, listed as 'colour transmitted' in Appendix A3.1. For example, if it is necessary to estimate the thickness of a film of SiO_2 grown on the surface of a single crystal of carborundum (SiC, silicon carbide) use the 'colour transmitted' list, because the refractive index of silicon carbide is greater than that of silica. In fact, silicon carbide is strongly absorbing over the visible spectrum and when first grown the crystals of carborundum are a shiny black. However, they soon take on a wide variety of attractive iridescent colours because of surface oxidation, which produces thin silicon dioxide surface films in a wide variety of thicknesses (Figure 3.11). These films are protective and preserve the underlying material from further oxidation, so that the colours only change slowly over the course of time.

Similar colours are seen on the surfaces of some metals due to oxidation. The film is usually of a transparent oxide, Al_2O_3 on Al, TiO_2 on Ti, Ta_2O_5 on Ta and so on. When they form as a result of the metal being used as an electrode in an electrochemical cell the metal is said to be *anodized*. These films, if of the appropriate thickness, will be brightly coloured. (Note that some anodized films are made especially thick to protect the underlying

Figure 3.11 ***Colours due to white light interference in a thin transparent film of silicon dioxide (SiO_2) on carborundum (SiC, silicon carbide). The colour variation is due to changes in film thickness***

metal. They are frequently coloured by the incorporation of dyes for decorative purposes. These colours are not thin film effects and arise from the dye molecules (Chapter 8).)

Thin-film colours are also frequently seen when an oil layer covers a puddle of water on a road, where the refractive index of the oil is usually greater than that of the underlying water. These colours are enhanced to the eye by the black road surface, which absorbs all light not reflected by the film. As the thickness of the oil changes in response to wind or water movement, the colours vary considerably.

In fact, the eye is able to detect minute changes in surface appearance when a thin film is deposited upon a substrate. As surprising as this may seem, the fastest and simplest way to detect single atomic layers of graphene is to use reflected white-light optical microscopy. Graphene, which is being actively studied because of its remarkable electronic properties, is composed of a single layer of carbon atoms linked in a hexagonal array – a single sheet from a graphite crystal, in fact. Graphene can be prepared by rubbing a graphite crystal over a smooth surface, a process called *mechanical defoliation*. A graphene layer on a such a substrate can be readily detected by eye because of the additional path difference introduced by the graphene layer, even though this is of only one atom in thickness, coupled with the fact that graphene absorbs a little of the incident light. Graphene sheets on silicon dioxide, for example, look transparent pale purple.

3.6 The Reflectivity of a Single Thin Film on a Substrate

The reflectivity of a single thin film deposited on a substrate, like that of a single thin film in air, depends upon the polarisation of the light, the film thickness and direction of the incident radiation. In the case of monochromatic illumination perpendicular to a homogeneous nonabsorbing thin film:

$$R = \frac{2r_1^2 + 2r_1 r_2 \cos 2\delta + r_2^2}{1 + 2r_1 r_2 \cos 2\delta + r_1^2 r_2^2}$$

where

$$r_1 = \frac{n_0 - n_\mathrm{f}}{n_0 + n_\mathrm{f}}$$

$$r_2 = \frac{n_\mathrm{f} - n_\mathrm{s}}{n_\mathrm{f} + n_\mathrm{s}}$$

n_0 is the refractive index of the surrounding medium, n_f is the refractive index of the film and n_s is the refractive index of the substrate. The expression for δ is:

$$\delta = \frac{2\pi[d]}{\lambda} = \frac{2\pi n_\mathrm{f} d}{\lambda}$$

where $[d]$ is the optical thickness of the film and d is the physical thickness of the film. For values of $[d]$ given by $\lambda/2$, λ, $3\lambda/2$, etc. the equation reduces to:

$$R = \frac{(n_0 - n_\mathrm{s})^2}{(n_0 + n_\mathrm{s})^2}$$

This is *identical* to the equation for an uncoated surface. Thus, a layer of optical thickness $\lambda/2$, etc. can be considered to be *optically absent* and the surface has normal uncoated reflectivity. This is an intriguing and useful result. It means that if a delicate surface is coated with a $\lambda/2$ layer of a hard transparent material the surface will be protected without any effect on optical properties.

For values of $[d]$ given by $\lambda/4$, $3\lambda/4$, etc. the reflectivity is given by:

$$R = \left(\frac{n_f^2 - n_0 n_s}{n_f^2 + n_0 n_s}\right)^2 \tag{3.2}$$

and the reflectance will be *either* a *maximum* or a *minimum*. This will depend upon whether the film has a higher refractive index than the substrate or a lower refractive index than the substrate. When the refractive index of the film is between that of the surrounding medium and the substrate ($n_0 < n_f < n_s$), the reflectivity will be a *minimum*. When the film has a *higher* refractive index than both the substrate and the surrounding medium ($n_0 < n_f > n_s$), the reflectivity will be a *maximum*.

As with a thin film in air, the value of the reflectivity will cycle with film thickness between a lower value at $[d]$ equal to 0, $\lambda/2$, λ, etc. to a maximum for values of $[d]$ equal to $\lambda/4$, $3\lambda/4$ and so on. Because the refractive indices are a function of wavelength, the reflectivity will also vary across the spectrum.

3.7 Low-Reflection and High-Reflection Films

3.7.1 Antireflection coatings

We can easily use the above equations to see how thin films modify the reflectivity of a surface. Suppose that it is desired to make a nonreflective coating on a glass surface in air. (Such coatings are called antireflection (AR) coatings.) Equation 3.2 shows that if the value of n_f lies between that of air and the glass then the reflectivity will be a *minimum* for a $\lambda/4$ film. Putting $R = 0$ in Equation 3.2 yields a value of the refractive index of the film which will give no reflection at all:

$$n_f = \sqrt{n_s} \tag{3.3}$$

For glass, n_s is about 1.5, so the antireflecting film must have a refractive index:

$$n_f = \sqrt{1.5} = 1.225$$

Very few solids have such a low index of refraction, and a compromise material often used is magnesium fluoride, MgF_2, for which n in the middle of the visible is 1.370 at 500 nm.[1] This is not perfect, but does reduce the reflectivity from about 4 % down to about 1 % (Figure 3.12). The coating will actually be maximally antireflective for the *design wavelength*, which is the wavelength for which the AR coating is optimised and the amount of light reflected will increase for wavelengths on either side of the design wavelength and also for oblique angles of incidence. For camera lenses, which commonly use AR coatings, the design wavelength is usually near the middle of the visible spectrum, say 550 nm. Such films reflect violet and red more than yellow or green; an effect readily observed when a good coated camera lens is examined.

[1] Note that MgF_2 is not isotropic and the refractive index depends upon crystal direction (see Chapter 4). In this and similar cases, the coatings are made by evaporation and generally have a single effective refractive index.

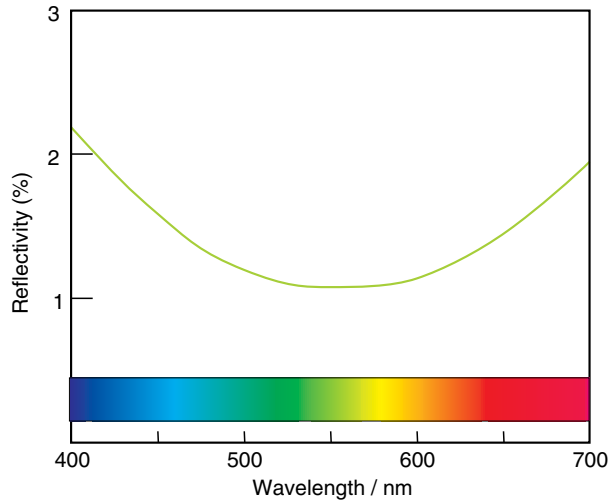

Figure 3.12 ***The reflectivity of a quarter-wave film of a magnesium fluoride (MgF_2) AR coating on a glass surface with a refractive index of 1.52. The design wavelength of the film is 550 nm and the beam is taken as perpendicular to the surface***

3.7.2 Antireflection layers

Apart from their utility as surface coatings, AR layers are also important in a variety of applications. For example, the fabrication of an integrated circuit on a silicon chip involves one or more steps in which the material is exposed to light through a pattern called a *mask*. The mask is used to selectively illuminate areas on the chip which, after further processing, build into the array of transistors which manipulate data. The light actually interacts with a layer of substance called a photoresist. After illumination the photoresist employed is weakened in those areas which were exposed to light and these are subsequently dissolved away so as to reveal the underlying silicon, which can then be selectively doped or otherwise treated. The length of time of the exposure of the photoresist to light is critical to the success of the process.

The desire to pack more and more transistors onto a chip has led to the drawing of ever finer detail onto the mask and the use of increasingly shorter wavelength light in the illumination steps. At present, the use of ultraviolet radiation is commonplace. The sharpness of the pattern produced on the silicon, and hence the number of transistors which can be placed onto the chip, is limited by diffraction (Chapter 6) and multiple reflections within the photoresist. The multiple reflections expose parts of the photoresist which should remain unexposed (Figure 3.13a). This has the effect of reducing the sharpness of the projected pattern and can also introduce spurious detail or defects.

In order to combat this difficulty an AR coating can be applied between the silicon substrate and the photoresist (Figure 3.13b). The aim is to introduce a film of the correct thickness to ensure that successive rays reflected at the bottom surface of the photoresist are out of phase by $\lambda/2$ so that destructive interference occurs in the photoresist layer. In terms of the AR layers previously discussed, the photoresist becomes the surrounding medium, refractive index n_0, the new layer is the AR layer, refractive index n_f, and the substrate remains as silicon, refractive index n_s.

Although the idea is conceptually simple, the thickness of the AR layer is rather difficult to determine. There are two main reasons for this. As the layer is interposed between the silicon and the photoresist the simple

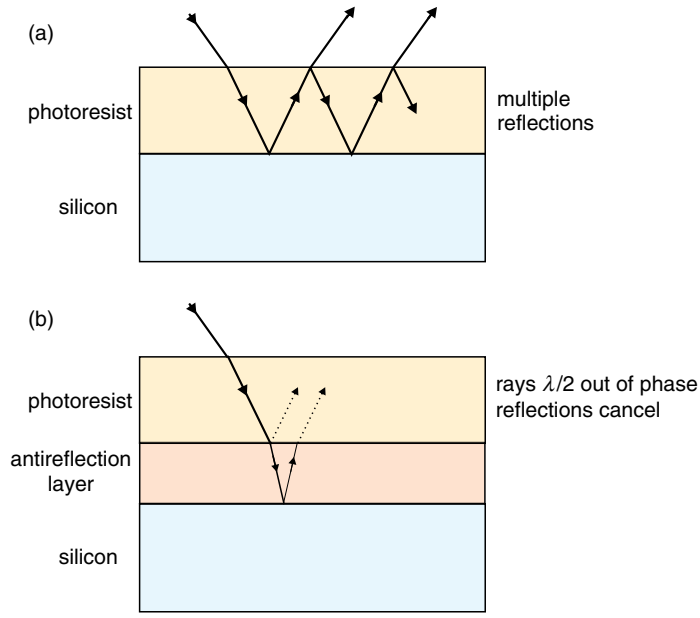

Figure 3.13 ***(a) Multiple light reflections in a film of photoresist on a silicon surface. (b) The deposition of an AR layer between the photoresist and the silicon results in cancellation of reflected beams by destructive interference, thus increasing the precision of the process***

formula in Equation 3.3 cannot be applied and rather complex calculations of the reflectivity must be made. Second, the simple refractive index term n of the layer must be replaced by the complex refractive index N, because at wavelengths in the ultraviolet region many materials which are transparent at visible wavelengths absorb strongly.

One suitable material that has been used in AR layers is silicon oxynitride, SiO_xN_y, often written as SiON. The compound has an advantage in that a change of composition alters the optical properties of the film (Table 3.1). The material is laid down as a thin film by passing a mixture of silane (SiH_4), nitrous oxide (N_2O) and nitrogen (N_2) over the silicon wafer. The various proportions of the gases control the composition and, hence, allow the wavelength at which the film is optimally antireflective to be varied at will. The SiO_xN_y layer is thus said to be a *tuneable* AR layer.

Table 3.1 ***Optical properties of Si–O–N films at 248 nm wavelength as a function of composition***

Composition	Refractive index n	Extinction coefficient k
$SiO_{0.86}N_{0.24}$	1.8948	0.4558
$SiO_{0.71}N_{0.27}$	1.9682	0.5253
$SiO_{0.54}N_{0.59}$	2.0821	0.5004
$SiO_{0.47}N_{0.49}$	2.2127	0.6030

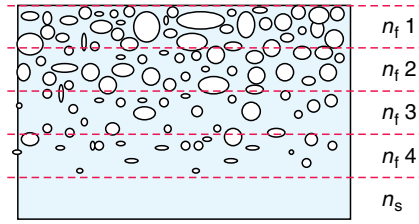

Figure 3.14 ***A surface foam can act as an AR coating. The reflectivity of the coating is determined by dividing up the surface into a large number of parallel layers and assessing the refractive index of each slice. The overall refractive index of the surface layers must equal the square root of the refractive index of the substrate for perfect AR behaviour***

3.7.3 Graded index antireflection coatings

The problem of forming a single-film AR coating on a surface is contained in Equation 3.3. In the case of glass it has not proved possible to find a film material with a refractive index that fits this equation exactly. One solution to the problem is to make a film in which the refractive index varies gradually from that of the surrounding medium, usually air, to that of the substrate; that is, a GRIN material (Section 2.5).

The first practical use of this idea, conceived more than 50 years ago, was to fashion a surface foam. The idea is to have a high concentration of air bubbles at the outer surface that gradually falls to zero at the inner (substrate) surface (Figure 3.14). Provided that the air bubbles are smaller than the wavelength of light, they are not resolved and the light encounters a medium in which the effective refractive index gradually increases from that of air to that of the substrate. Porous coatings of this type can be made from a silica gel. If a glass surface is dipped into the gel and then heated to form a porous glass layer, an antireflective surface coating can be formed which fits Equation 3.3 precisely.

The refractive index of the film will depend upon the volume and size distribution of the pores, the polarisation of the incident light and will be wavelength dependent. To a first approximation, the assumption that the material behaves as a simple mixture (Section 2.5) can be employed. The average refractive index of the whole film is then given by Equation 2.11, which is also written in the form:

$$n_f = n_0 + F(n_s - n_0) \tag{3.4}$$

where n_0 is the refractive index of the surrounding medium, which also fills the pores, usually air, with $n_0 = 1$, and n_s is the refractive index of the substrate; the amount of solid in the antireflecting layer is called the filling factor F (identical to the volume fraction of substrate V_s), which runs from 0 % at the surface to 100 % at the substrate.

The idea of using GRIN optics in AR coatings, albeit in a slightly different form, was evolved in night-flying insects some millions of years ago. It is clearly of advantage to optimize the amount of light that the eyes of these night-flying insects receive and an AR coating on the eyes helps in this. The AR coating derives from the normal surface architecture of the insect eye. Adult insects use compound eyes, each of which is formed of many separate imaging units called *ommatidia*. The ommatidia form a hexagonal pattern of facets on the surface of the eye, each facet corresponding to the outer surface of an ommatidium. The eye facets of most day-flying insects, such as bees and dragonflies, are smooth, but certain night-flying moths and a few butterflies have facets that are covered with tiny bumps (Figure 3.15). The dimensions of the bumps are about half the wavelength of light, being about 200 nm at the base and 200 nm high. These bumps form an effective GRIN layer that endows the surface of each facet with marked AR properties.

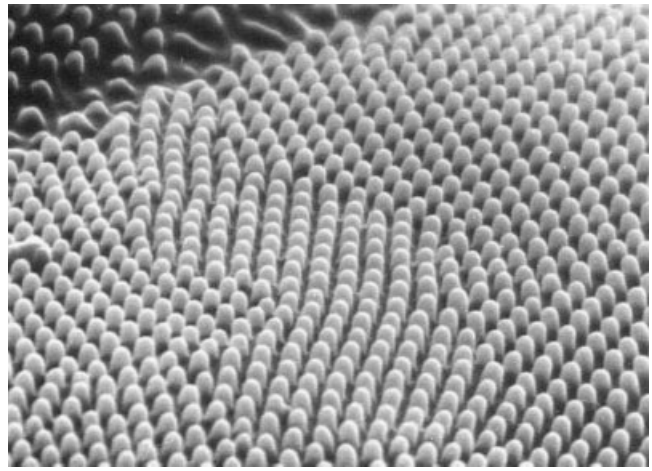

Figure 3.15 ***The antireflective GRIN structure on the surface of the eye of Morpho butterfly. [Reprinted by permission from Macmillan Publishers Ltd: NATURE, Photonic structures in biology, Pete Vukusic and J. Roy Sambles, 424, 852–855, copyright (2003)]***

In order for the moth-eye surface to act as an AR layer, the protuberances must be small enough not to be resolved by light, which means in practice that the bumps must be separated by half the wavelength of the light or less. If this is not so, the array will act as a diffraction grating (Chapter 6). The surface architecture must also not be confused with surface roughness, which will increase diffuse reflection compared with specular reflection, but not decrease the total amount of light returned towards the source. The antireflective properties of moth-eye surfaces can be determined by dividing the bumpy surface into slices parallel to the substrate surface, estimating the average refractive index and reflectivity of each layer and then summing over the slices to determine the reflectivity of the whole structure (Figure 3.16). This is a complex calculation, as the polarisation of the light must be taken into account. However, an approximate estimation of the effective refractive index can be made using Equation 3.4. (An alternative approach via a diffraction problem is given in Section 6.2.) These bumpy surfaces are now being reproduced artificially for use as AR coatings. As the effect was first recorded on the surface of the eyes of some moths, these types of surface AR coating are called *moth-eye AR coatings*. The more formal name for a moth-eye AR coating is *ultrahigh spatial-frequency surface relief grating*.

Nanoparticles can be used in a similar fashion. The refractive index of a layer of nanorods depends upon the constituents of the rods, the spacing between them and the angle at which they lie on the surface. The use of

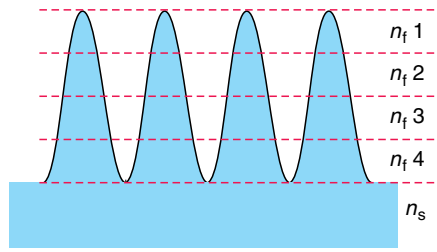

Figure 3.16 ***A moth-eye surface structure can act as an AR coating. The reflectivity of the coating is determined by dividing up the surface structure into many thin layers and assessing the refractive index of each slice. The overall refractive index of the surface layers must equal the square root of the refractive index of the substrate for perfect AR behaviour***

several layers of rods can thus make a GRIN surface layer. The best AR coating (2009) has been made from five 100 nm layers of silica and titanium dioxide nanorods deposited at 45° to the surface of aluminium nitride plates, a material of use in LEDs and semiconductor lasers. The final layer, with an effective refractive index of 1.05, gives a reflectivity of 0.01 % (see this chapter's Further Reading).

3.7.4 High-reflectivity surfaces

Thin-film coatings can also be used so as to optimize the reflectivity; that is, make the value of R as close to unity as possible. A film of thickness $\lambda/4$ will achieve this provided that the refractive index of the film n_f is greater than both n_0 and n_s. Two materials frequently used are SiO_x, with x approximately equal to 1.0 ($n \approx 2.0$), and TiO_2 ($n \approx 2.5$–2.8). A TiO_2 film of thickness $\lambda/4$ on glass will have a reflectivity of about 0.40 (40 %). As R for a single glass surface in air is about 0.04 (4 %), 40 % represents a tenfold improvement. The effect is used in costume jewellery. Rhinestones consist of a glass object with refractive index close to 1.52 coated with an approximately $\lambda/4$ thickness film of TiO_2. Variations in film thickness and viewing angle give these objects a wide variety of fleeting colours which are meant to simulate the fire of diamonds. Sparkling paints and nail varnish also make use of an approximately quarter-wavelength thickness of TiO_2 deposited onto flakes of mica which are subsequently dispersed in the product. The various colours seen are created in a similar way to the colours on rhinestones.

3.7.5 Interference-modulated (IMOD) displays

Thin film interference is able to generate bright remarkably colours. This is exploited in a display technology aimed at mobile phone screens. The idea is based on the interference of white light falling on a pair of parallel reflecting surfaces, so that colour is essentially developed in a thin air film. The arrangement is similar to that of a *Fabry–Pérot étalon*. This device, which is an interferometer, consists of a semitransparent film separated from a fully reflecting film by a narrow air gap. Light from a broad source falling on the top surface is repeatedly reflected from the bottom surface and leaks from the top surface as a reflected beam and from the bottom surface as a transmitted beam. In a classic Fabry–Pérot étalon the transmitted beam is exploited and the reflected beam is suppressed. In an IMOD display the reflected beam is exploited.

The arrangement of a single pixel consists of a pair of mirrors separated by a narrow air gap (Figure 3.17a). The principle of operation is as given in Sections 3.2 and 3.3. The pixel will reflect light of a wavelength λ brightly for incident light falling normal to the surface when:

$$2d = (m + \tfrac{1}{2})\lambda$$

where d is the separation of the mirrors and m is an integer. As the viewer moves away from normal incidence the colour will appear to move to shorter wavelengths; that is, red tends to move towards blue. The actual colour of the pixel will not be a single wavelength, of course, but will depend upon the interference of the whole spectrum, as described above (Figure 3.10).

The device can operate in an interactive fashion if the separation of the air space between the mirrors is varied according to a controlled input. In current displays this is achieved by using electrostatic attraction between the top (fixed) and lower (moveable) film. Piezoelectric movement, used to control electrodes in a number of devices, including surface tunnelling microscopes, which are able to reveal atomic features on a surface, can also be utilized. As the separation varies, so the colour of the pixel changes (Figure 3.17b). These displays are currently being widely explored for mobile telephone screens. They have an advantage in that although power is needed to change the colour of a pixel, once that colour is set, no power is needed to maintain it. In competing

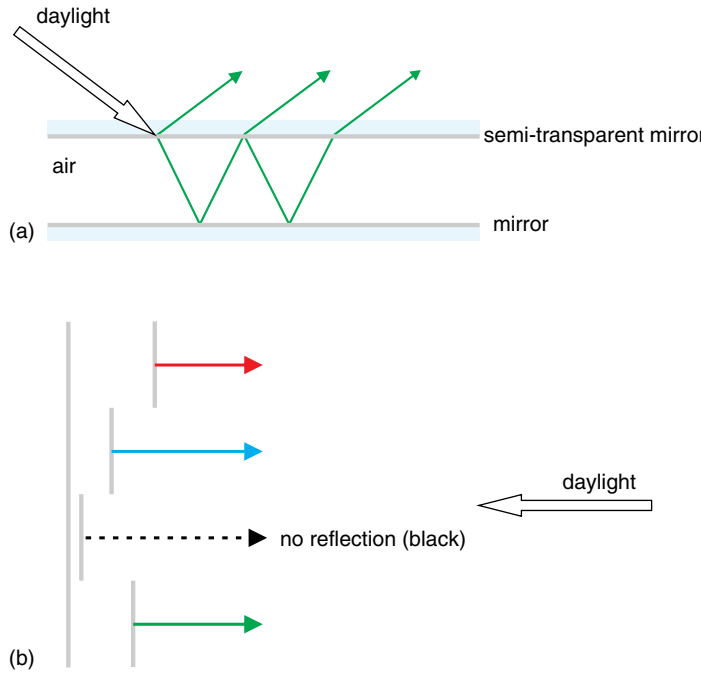

Figure 3.17 ***The principle of operation of an IMOD display: (a) reflection of light from a pair of parallel mirrors (a Fabry–Pérot etalon); (b) variation of mirror separation gives rise to different coloured pixels***

technologies, such as liquid crystal displays or organic light emitting diode displays, the power must be supplied continuously to maintain colour and brightness. Moreover, these pixels are easily visible in bright daylight, which is a drawback of some present displays.

3.8 Multiple Thin Films

3.8.1 Dielectric mirrors

Traditionally, mirrors have been made from metals. The best metallic mirrors are made of a thick layer of silver, which has a reflectivity of about 0.96 in the visible. (The reflectivity of metals is considered in more detail in Section 10.15.) Surprisingly, multiple thin films of transparent materials can be laid down one on top of the other in such a way as to form perfect mirrors. These are often called *dielectric mirrors*. The fabrication of such devices forms part of the subject area known as *photonic* or *thin-film engineering*. A wide variety of multilayer mirrors are now manufactured, mainly from oxides and fluorides. These are all stable in air and have the additional advantage over metallic mirrors of not degrading in normal use.

The simplest formula for the reflectance of such a mirror refers to the specific case in which all layers are $\lambda/4$ thick and of alternating high (H) and low (L) refractive indices, n_H and n_L, illuminated by light falling *perpendicular* to the surface. The arrangement (Figure 3.18) is called a *quarter-wave stack*. The maximum reflectance of a quarter-wave stack deposited on a substrate in the sequence:

substrate; L, H; L, H; L, H; . . . L; H; air

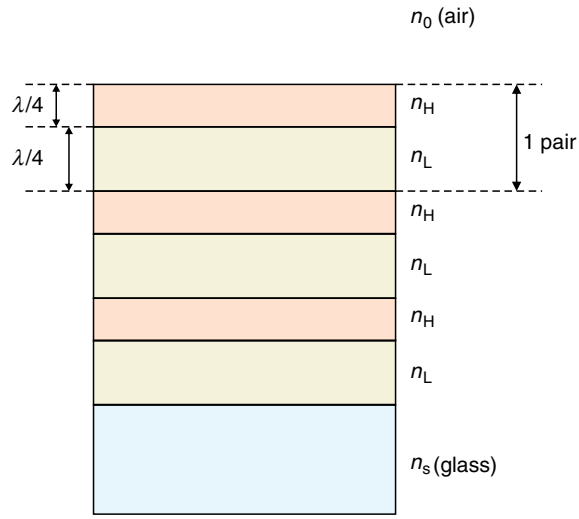

Figure 3.18 ***A stack of thin films, each of optical thickness λ/4, called a quarter-wave stack, can act as an effective dielectric mirror. The reflectivity increases with the number of pairs of layers and rapidly approaches 1.0***

is given by the formula:

$$R = \left(\frac{n_s f^{2N} - n_0}{n_s f^{2N} + n_0}\right)^2$$

where f is equal to (n_H/n_L), n_0 is the refractive index of the surrounding medium, usually air ($n_0 = 1.0$), n_s is the refractive index of the substrate, usually glass ($n_s \sim 1.5$) and N is the number of (LH) *pairs* of layers in the stack.

For a stack in air this equation is equivalent to:

$$R = \left(\frac{n_s f^{2N} - 1}{n_s f^{2N} + 1}\right)^2 = \left[\frac{n_s - (n_L/n_H)^{2N}}{n_s + (n_L/n_H)^{2N}}\right]^2$$

Computation shows that, as the number of pairs of layers increases, R rapidly approaches 1.0, implying perfect reflectivity.

The form of the reflectivity as a function of wavelength for light falling on the stack at normal incidence has a typical structure consisting of a central plateau together with small side maxima distributed about the design wavelength λ_0 (Figure 3.19). In general, the central plateau becomes squarer and higher as the number of layers increases until a reflectivity of unity is reached. The width of the central plateau is given by:

$$\Delta\lambda = \frac{4\lambda}{\pi} \arcsin\left(\frac{1-f}{1+f}\right)$$

where $f = (n_H/n_L)$.

Different formulae must be used if the stack terminates with an L-layer, if there are not complete sets of pairs of layers or for oblique illumination. When the beam is at an oblique angle of incidence the polarisation of the beam must also be taken into account.

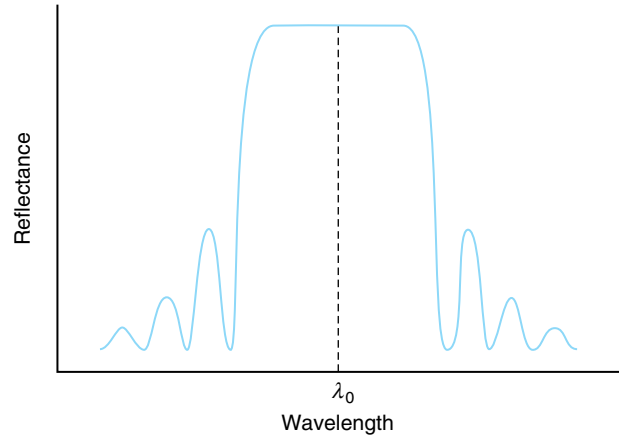

Figure 3.19 ***General form of the reflection from a quarter-wave stack as a function of the wavelength for light at normal incidence***

3.8.2 Multilayer stacks

The difficulty of making calculations of the reflectivity and transmissivity of thin-film multilayers prevented large-scale use of this technology in the first half of the twentieth century. The mathematical formulation of the problem, though, was solved at this time, and the optical properties of a stack can be described by a methodology that allows the contribution of each layer to be represented by a matrix. The total optical effect of the stack is obtained by multiplying the matrices together. Suitable computational software is now readily available (see this chapter's Further Reading).

The general approach used to make a multilayer optical component is to lay down a stack of thin films which have alternately higher and lower refractive indices using vacuum evaporation of the materials. Manipulation of the thicknesses and the refractive indices of the layers in the stack, in accordance with computation, allows for the modification of the optical properties at will. This technology is thus equally suitable for the production of multilayered AR coatings. For example, Figure 3.20a–d shows the variation in reflectivity of a stack of four thin films as the thickness of just one of the layers is changed. The four thin films are deposited on a glass substrate and alternate between high refractive index (H) and low refractive index (L), ending with air. The arrangement of the layers is: air ($n = 1.0$); (1) L, 93 nm, $n = 1.48$; (2) H, 120 nm, $n = 2.30$; (3) L, 37 nm, $n = 1.48$; (4) H, variable thickness, 30 nm, 24 nm, 18 nm, 12 nm, $n = 2.30$; substrate, glass, $n = 1.52$. The single layer to be changed was that next to the glass substrate, and then only from a thickness of 30 nm to 12 nm. The curves are all evaluated for a design wavelength of 550 nm and for light normally incident upon the stack. The final curve (Figure 3.20d) makes an almost optimal AR coating.

In general, when a multilayer stack is tilted the reflectivity must take into account polarisation. Although this has only a small effect on the total reflectivity, the wavelength which is strongly reflected or transmitted shifts towards lower values, but it does so much more slowly than for a single thin film. Thus, the film will look bluer as the stack is tilted.

It is found that the central wavelength will decrease from λ_0 for normal incidence to λ_θ when the stack is tilted through small angles θ (than 20°) given by the expression:

$$\lambda_\theta = \lambda_\theta[1-(\theta^2/2n_f^2)]$$

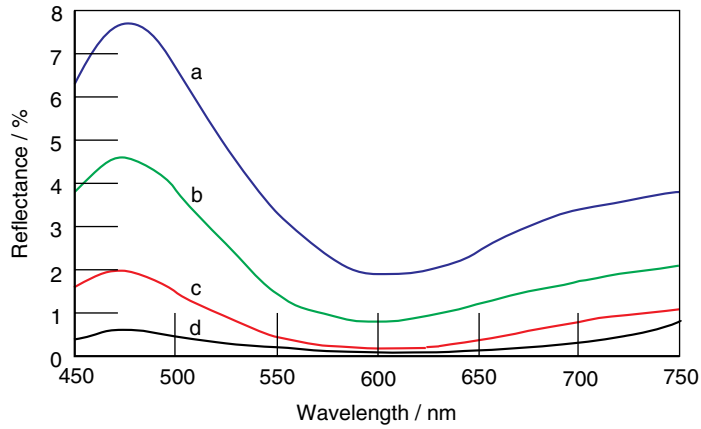

Figure 3.20 ***The reflectivity of a stack of four thin films on a glass substrate in air. The thickness of each layer is constant except for the one adjacent to the glass, which takes values of (a) 30 nm, (b) 24 nm, (c) 18 nm, (d) 12 nm. The stack (d) shows almost perfect AR behaviour. Computations were made using 'Filmstar' software (see this chapter's Further Reading)***

where n_f is the effective refractive index of the stack and θ is in radians. This means that these multilayer stacks are *tunable* over small degrees of rotation. For accurate work the stack must be aligned precisely to ensure wavelength-specific performance.

If the layers are uneven in thickness, or to some extent disordered, a wide variety of wavelengths will be reflected. These will be perceived as white or silver, depending upon the smoothness of the surfaces. This is the reason why a roll of thin plastic film used for food wrap looks silver. Many insects show silver markings that are similarly made up of thin layers of transparent material of varying spacings (Figure 3.21).

3.8.3 Interference filters and distributed Bragg reflectors

The same technique of multiple dielectric layer deposition can be used to make *interference filters*. The form of the reflection curve of a multilayer stack (Figure 3.19) shows that wavelengths to either side of the central plateau will be transmitted and those within the plateau will be reflected. By using multiple thin films the regions that transmit or reflect can be precisely manipulated to make optical filters. These fall into three different categories. *Shortpass filters* transmit visible wavelengths and cut out infrared radiation (Figure 3.22a). They are often used in surveillance cameras to eliminate heat radiation. *Longpass filters* block ultraviolet radiation and transmit the visible (Figure 3.22b). Other filters, called *bandpass filters*, pass only a limited section (or band) of the electromagnetic spectrum (Figure 3.22c). (These thin-film interference filters generally give a much sharper transmittance than the type of filter made from dye molecules distributed in a gelatine matrix; the type of filter illustrated in Figure 1.18). As the filters are made of transparent layers, the wavelengths not transmitted are reflected. Bandpass filters, therefore, act as mirrors for the complementary colour of the transmitted band. Because of this effect, these filters are often vividly coloured (Figure 3.23).

When multilayer reflectors are included in an optical device such as a waveguide or some types of laser they are called *distributed Bragg reflectors*. They are typically made from layers of TiO_2 and SiO_2. The reflectivity of such a multilayer is computed in the same way as any multilayer stack, taking into account the surroundings

Figure 3.21 ***The Silver-washed Fritillary butterfly, Argynnis paphia. The silver 'wash' on the wings is caused by reflection from a disordered thin-film multilayer stacks***

and the substrate on which the Bragg reflector is deposited. The wavelength interval that is reflected from such a reflector is called the *photonic stopband*. The approximate width of the stopband is given by the formula:

$$\Delta\lambda = \frac{4\lambda}{\pi}\arcsin\left(\frac{1-f}{1+f}\right)$$

where $f = n_H/n_L$.

3.9 Fibre Bragg Gratings

Multilayer interference filters can also be produced in the cores of optical fibres. These are called *fibre Bragg gratings* (FBGs) and are used for controlling light signals as they travel along the fibre. FBGs are formed within the core of an optical fibre (usually a monomode fibre) (Section 2.9) in which the refractive index is modulated in a periodic way with a repeat spacing d of about the wavelength of light.

The formation of an FBG was first observed in 1978, more or less by accident, rather like the initial observation of the formation of frequency-doubled light in a fibre (Section 4.11). Light from an argon-ion laser was focused into a length of germanium dioxide (GeO_2)-doped silica (SiO_2) fibre and, surprisingly, more and more light was reflected back along the fibre as time passed. It was concluded that a refractive index grating was being created in the fibre by interference between the incident wave and a wave reflected from the far end of the fibre. The two waves formed an interference pattern in the fibre, which produced the refractive index change. Although initially treated as a bizarre phenomenon, it has since been found that any GeO_2-doped SiO_2 fibre will behave in a similar fashion. The refractive index gratings that form in this way are called *Hill gratings*. Hill gratings are limited to the wavelength of the radiation producing the effect.

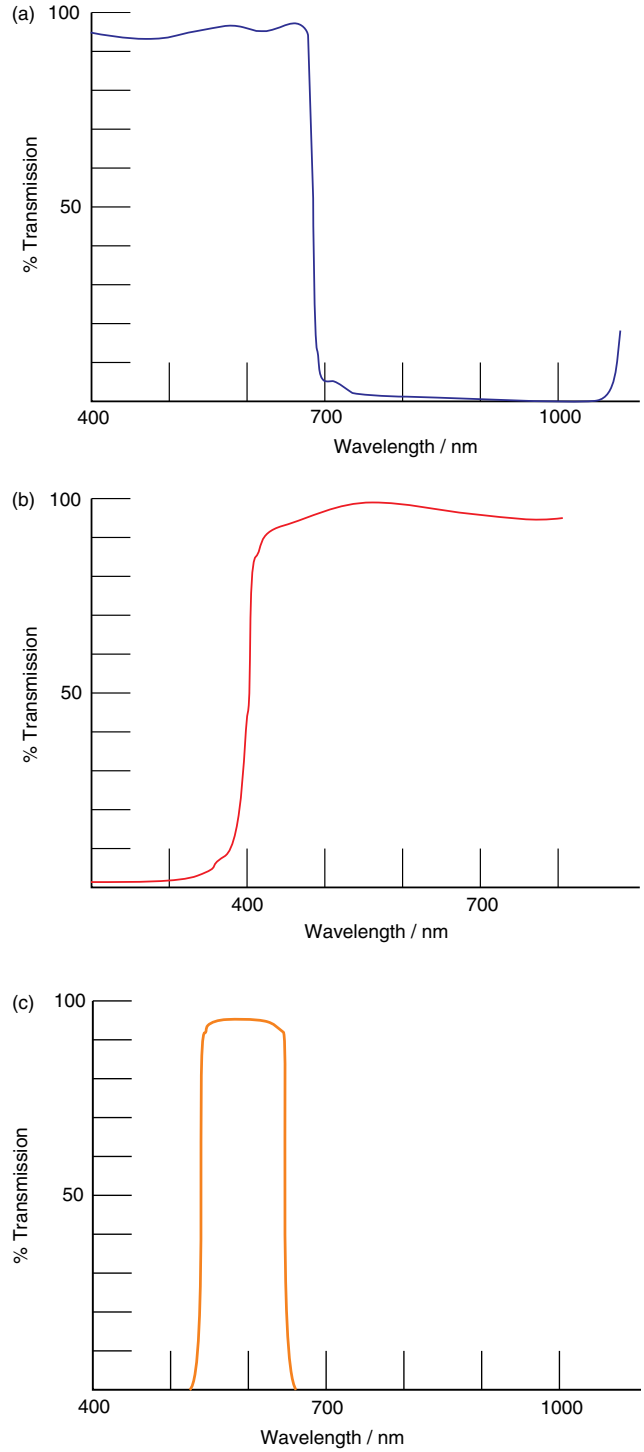

Figure 3.22 ***Transmission profiles of multilayer dielectric filters: (a) a shortpass filter; (b) a longpass filter; (c) a bandpass filter***

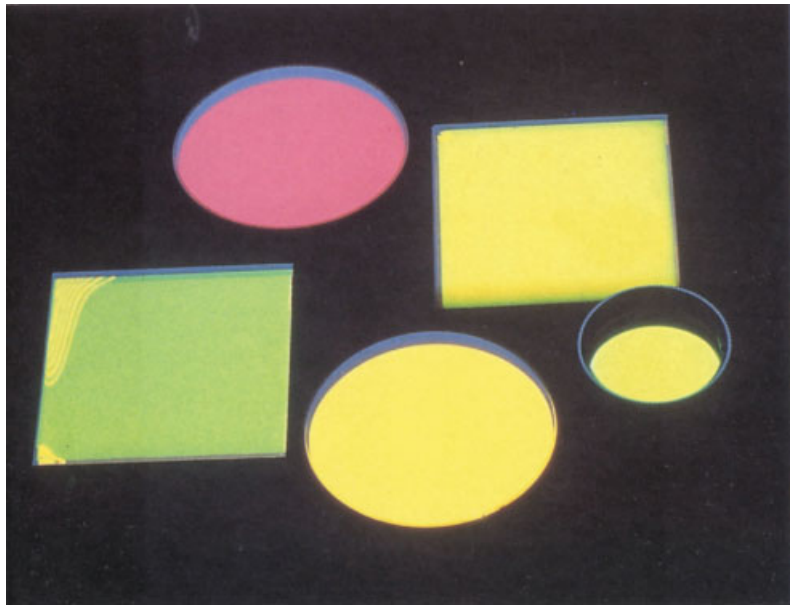

Figure 3.23 ***Multilayer interference filters. The bright reflected colours are complementary to the colours transmitted by the filters and absorbed by the black backing***

The simplest (conceptual) modulation is a step repeat (Figure 3.24). This type of grating is described as a *uniform grating*. If the spacing of the refractive index modulation is not constant, but varies in spacing in a uniform way along the length of the modulation from d_1 to d_2, the grating is said to be *chirped*. All can be described as a form of *distributed Bragg reflector* (Section 3.8).

The way in which FBGs influence light pulses passing down the core of the fibre can be understood in terms of multiple thin-film optics. The light will be reflected back from the grating if the wavelength of the light λ and the spacing of the grating d are given by:

$$\lambda = 2n_{\text{av}}d$$

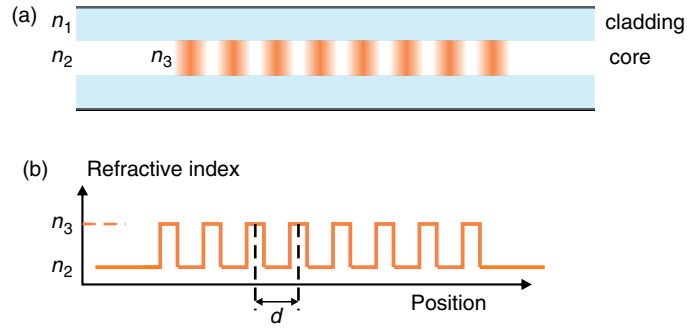

Figure 3.24 ***FBGs. (a) Periodic modulation of the refractive index in the core of an optical fibre. (b) The simplest step modulation of refractive index. The refractive indices of the cladding, core and modified core are n_1, n_2 and n_3 respectively***

where n_{av} is the average of the refractive index of the core and the modulated region. The value of the refractive index change Δn between the modulated and unmodulated regions is of the order of 10^{-3} to 10^{-4} on the core refractive index, which is close to 1.5. It is clear, therefore, that a single modulation would hardly cause any change in a pulse. However, FBGs are often of the order of 40 000 modulations in length (which only occupies 200 nm of fibre for blue–green light of 500–nm wavelength) and, hence, considerable intensity can be reflected. A pulse of white light introduced into a fibre containing such a grating would reflect back a pulse of monochromatic blue–green light of 500 nm wavelength. The other wavelengths would be transmitted. The grating is thus able to act as a filter or as a mirror, as in the case of the other multiple thin-film devices.

There are a number of ways of fabricating FBGs. The simplest is to use the interference of two ultraviolet laser beams shone onto the fibre from the side. The peaks and troughs of the interference pattern of two beams focused on the fibre create the refractive index changes required (Figure 3.25a). Because the spatial frequency of the interference pattern is readily changed by altering the angle at which the beams meet, a wide range in the spacing of the refractive index modulations can be imposed upon the core. Gratings can also be created by using a mask, which, because of the dimensions involved, acts as a diffraction grating to create a pattern of maxima and minima in the fibre core (Figure 3.25b). If the part of the fibre which lies in the interference pattern is bent into a curve, chirped gratings can be made.

As described above, FBGs form under the influence of external radiation, most often of ultraviolet frequencies. However, not all fibres are susceptible to the formation of refractive index gratings. The glass must be photosensitive; that is, they react to light in a specified way (see also Sections 10.17 and 10.18). Although GeO_2-doped SiO_2 glass is satisfactory, much better gratings form in fibres which also contain boron

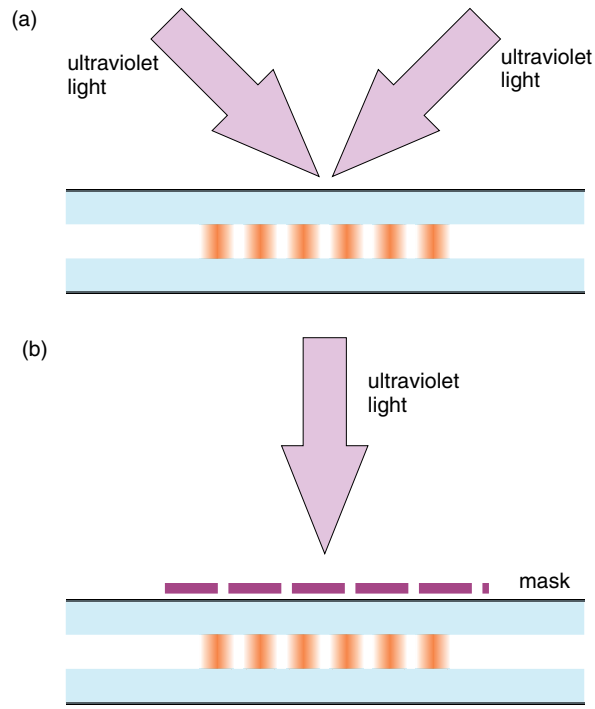

Figure 3.25 ***Fabrication of FBGs: (a) interference of two beams of ultraviolet light; (b) diffraction pattern from a mask***

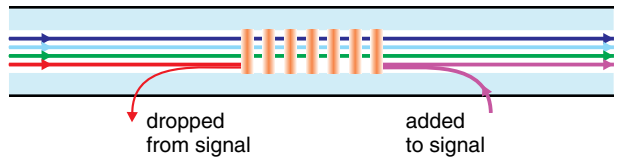

Figure 3.26 ***The addition and removal of a signal from a fibre using an FBG; schematic***

trioxide (B_2O_3) or tin dioxide (SnO_2) as co-dopants. Additionally, fibres can be transformed into a photosensitive state by forcing hydrogen into the structure.

There is some uncertainty about the mechanism by which the change in refractive index is produced. It is agreed, though, that defects in the structure are involved in some way. From a number of possibilities, local density variation, the formation of colour centres involving GeO or the formation of centres involving a germanium–hydrogen (GeH) pair seem to be the most likely candidates at present.

There is considerable interest in FBGs because they have numerous applications in fibre-optic communications. Clearly, each different wavelength that passes down a cable can carry data. As colour signals do not become mixed, the more wavelengths that can be crammed into a fibre the more data that it can carry per unit time. The technique of putting large numbers of different wavelengths down a fibre is called *dense wavelength division multiplexing* (DWDM). In this context, FBGs can be used for adding or removing signals from a fibre, necessary in wavelength multiplexing of optical communication systems (Figure 3.26).

3.10 'Smart' Windows

Smart windows are those that respond to changes in the external and internal environment. There are a number of different types under active investigation. Here, just two are mentioned, both of which rely on thin-film reflectivity for the active function, low-emissivity windows and self-cleaning windows. For other approaches see Section 10.12.

3.10.1 Low-emissivity windows

Windows in buildings are targets for improved energy efficiency. The reason for this is that normal window glass is an extremely good absorber and emitter of thermal energy. The black-body equations (Section 1.6) show that a room with a temperature of 21 °C has approximately 94 % of the thermal energy in the range 5–40 μm, with a peak at about 10 μm. Glass absorbs and re-emits about 80 % of this energy, making windows an appreciable gateway for loss of heat. Windows which address this problem are known as *low-emissivity* windows.

The details depend upon the place of use. In colder regions it is not only necessary to minimize heat loss to the outside, but also to guarantee that solar energy penetrates the glass and acts as a passive heating agent. In desert regions it might be more desirable to make reflection of external solar energy the priority.

All the systems in use rely on coating the inside of one or both panes of a double sheet of glass with a thin film of material which, in simple terms, is transparent to visible wavelengths and opaque to infrared. The positioning of the coating depends upon the use for which the window is designed. To prevent heat loss from rooms in cooler climates the coating is frequently upon the inside of the inner pane (Figure 3.27a).

One commonly used substance is tin dioxide (SnO_2) doped with fluoride ions (F^-), with a refractive index of approximately 2.0. This material is transparent to visible wavelengths but strongly absorbent to the wavelengths that characterize the thermal energy from the room, thus capturing the energy. These films have a

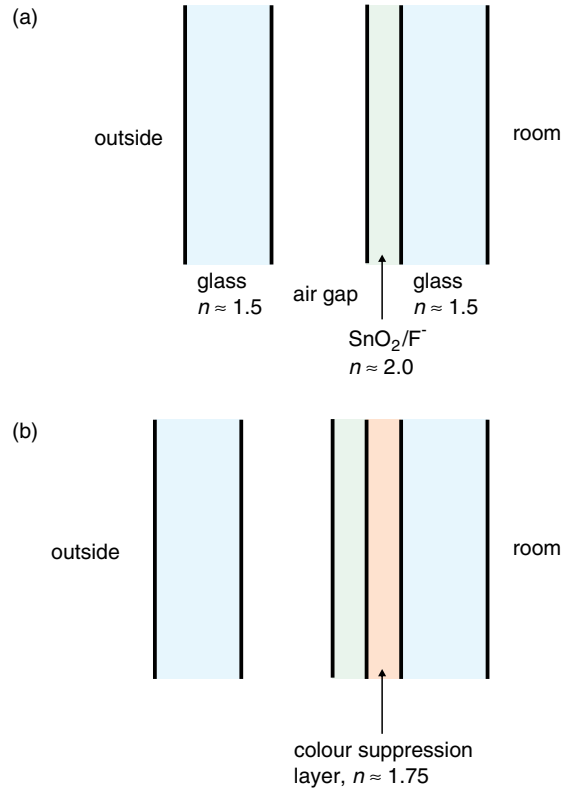

Figure 3.27 ***Low-emissivity coatings: (a) the coating is applied to the inside of a double glass unit and on the side nearest to the room; (b) another thin film with a lower refractive index is often applied to reduce reflections and act as a colour suppression layer***

low emissivity for these wavelengths and, hence, cannot lose the energy by radiation. The energy is conducted back through the glass and returned into the room by radiation from the uncoated surfaces. The useful performance of the film is limited by its thickness. As films become thicker, the emissivity increases, so it is important to keep film thickness low.

Unfortunately, the ideal thickness for SnO_2 films is exactly that which produces a green colour due to interference and gives green-tinted windows. The green reflection from the doped SnO_2 layer can be suppressed by coating the glass with a thin layer of transparent material with a lower refractive index than the SnO_2 before the SnO_2 is applied (Figure 3.27b). Colour suppression occurs via the same principles outlined in Section 3.7.2. The aim is to cause reflections from the top and bottom surfaces of the doped SnO_2 layer to be out of phase and so interfere destructively, hence eliminating colour production via interference. If the film is viewed from inside the room, to a first approximation it is convenient to call the glass pane the surrounding medium, refractive index n_0, and the doped SnO_2 coating as the substrate. Using the formula for a $\lambda/4$ AR layer, Equation 3.2, shows that the ideal film refractive index n_f is given by:

$$n_f = \sqrt{n_0 n_s} \tag{3.5}$$

where n_0 is the refractive index of the doped SnO_2 layer and n_s is the refractive index of the glass ($\sim$1.5). This suggests that a thin film with a refractive index which is of the order of 1.75 might form a suitable colour

suppression layer for someone inside the room. Exact multiple thin-film calculations are needed to refine the thin-film characteristics, both in reflection and transmission.

3.10.2 Self-cleaning windows

Self-cleaning windows need to destroy organic molecules and bacteria that stick to the glass. An additional desirable property is that the surface should be hydrophilic so that water flows over it readily and allows debris to be washed away with rain. Titanium dioxide (TiO_2) is an oxidation photocatalyst. It is able to decompose organic molecules and disrupt the surfaces of bacteria when irradiated with ultraviolet light. This has made it a promising surface coating for 'self-cleaning' widows, as normal sunlight contains sufficient ultraviolet to effect the removal of organic deposits on window surfaces over the course of the day. Moreover, thin films of TiO_2 pick up hydroxyl (OH^-) groups on the surface, making it hydrophilic. Thus, self-cleaning windows use external coatings of TiO_2.

As with low-emissivity windows, the thin film causes unwanted interference effects. In this case, the presence of a $\lambda/4$ thin film of TiO_2 on the window increases surface reflectivity greatly. This is given by Equation (3.2):

$$R = \left(\frac{n_f^2 - n_0 n_s}{n_f^2 + n_0 n_s}\right)^2 \tag{3.2}$$

where n_f is the refractive index of the TiO_2 film, n_0 is the refractive index of air (1.0) and n_s the refractive index of the window glass ($\sim$1.5). There are two common forms of TiO_2: anatase, with an effective refractive index in thin film form of approximately 2.52, and rutile, with an effective refractive index in thin film form of approximately 2.76. Substituting these into Equation 3.2 shows that the reflectivity of the surface will lie between approximate values of 38 and 45 %. Both of these are too high for convenient use in ordinary windows.

It is possible to try to suppress this high reflectivity by the inclusion of an AR coating between the TiO_2 film and the glass. However, this faces the same problem as described above for low-emissivity windows, and it is not easy to find a film that suppresses high reflectivity when viewed from both sides of the glass. GRIN techniques can help. Self-cleaning windows fabricated with a surface coating of porous silica about 120 nm thick containing nanoparticles of TiO_2 are able to combine both the self-cleaning and AR properties in one. As described above, a $\lambda/4$ AR layer on glass should ideally possess a refractive index of about 1.225 (Section 3.7.1). Porous silica can give a lower value than this, which is increased by the presence of the TiO_2 nanoparticles. The refractive index of the film can be calculated using the methods in Section 2.5, that is:

$$n_f = n_1 V_1 + n_2 V_2 + n_3 V_3 + \cdots$$

where n_1 represents the refractive index of component 1, etc. and V_1 represents the volume fraction of the material 1, etc.:

$$V_1 + V_2 + V_3 + \cdots = 1$$

In practice one would use computer software to evaluate the ideal thicknesses of the TiO_2 and SiO_2 (or other) AR layers so as to optimize the transparency of the window.

3.11 Photonic Engineering in Nature

The application of multiple thin films in nature is widespread, and a volume could easily be written on this topic alone. If the film thicknesses are fairly uniform, then a bright colour will be reflected. Such colours are generally

referred to as iridescent, meaning that the colour has a metallic appearance and the tone changes with viewing angle. If the layers are uneven in thickness, or to some extent disordered, a wide variety of wavelengths will be reflected. These will be perceived as white or silver, depending upon the smoothness of the surfaces (see Figure 3.21). All of these are referred to as structural colours to differentiate them from colours produced by pigments. Here, just a few examples from a legion are touched upon. Many more will be found if the references (see this chapter's Further Reading) are consulted.

3.11.1 The colour of blue butterflies

An example of the vivid blue colouring seen in butterflies is provided by the Common Blue, *Polyommatus icarus* (Figure 3.28a). The colour arises in tiny scales that cloak the wings (Figure 3.28b). The colour perceived is built up by a mosaic of these tiny scales and is similar in result to that used by pointillist painters such as Seurat. The blue scales of this butterfly are made up of sheets of transparent multilayers running parallel to the scale base (Figure 3.29a). There are four layers of transparent material with a thickness of about 50 nm and a refractive index of about 1.57 separated by air layers of approximately twice this dimension. In addition, the layers of transparent material are be perforated into a 'pepper-pot' structure (Figure 3.29b). Calculation confirms that this arrangement is highly reflective for violet–blue wavelengths.

In nature, there are many similar species of blue butterfly, each of which is characterized by a different tone of blue and which can be recognized one from another by these subtle differences. It is easy to appreciate that the colour of the reflective scales can be tuned by small changes in the multilayer thickness, spacing and degree of perforation. This latter attribute is equivalent to a GRIN layer that has a refractive index somewhere between that of air and 1.57.

3.11.2 Shells

Many shells have a multilayer construction, as this affords the desirable combination of strength and lightness. Occasionally this feature gives rise to structural iridescent colours. The colours are more often visible on the inside of a shell, as the outsides tend to be camouflaged or otherwise coloured to aid concealment. In many species these colours are pale greens and pinks and are known as mother-of-pearl or nacre. However, the New Zealand paua, *Haliotis iris*, has a very marked iridescence and displays intense colours that change with viewing direction (Figure 3.30). The colours exhibited are many vivid blues and greens. The multilayers giving rise to this spectacular effect are derived from alternating organic and inorganic layers. The colour effect is enhanced by dark-pigmented underlying material that absorbs any light that has not been reflected. The shells are used for decoration and jewellery.

3.11.3 Labradorite

Minerals can develop as multilayer structures in a number of ways. An example is provided by the mineral *labradorite*. This material exhibits flashing rainbow-like colours which vary as the angle of observation changes in a typically iridescent fashion (Figure 3.31). The phenomenon is also known as *schiller* and *labradorescence* when applied to the mineral. Most commonly the colours exhibited are violets and blues, but greens, yellow and orange colours can also be seen in some specimens.

Geologically, labradorite is a plagioclase feldspar; feldspars being minerals constructed from a strong framework of corner-sharing $(SiO_4)^{4-}$ groups with alkali or alkaline earth cations contained in the cages present. It has a composition lying between the parent compounds anorthite ($CaAl_2Si_2O_8$) and albite ($NaAlSi_3O_8$), both of which are also feldspars. Labradorite consists of between 50 % and 70 % anorthite, so that its formula can be written as $Ca_{0.5–0.7}Na_{0.5–0.3}(Al,Si)AlSi_2O_8$.

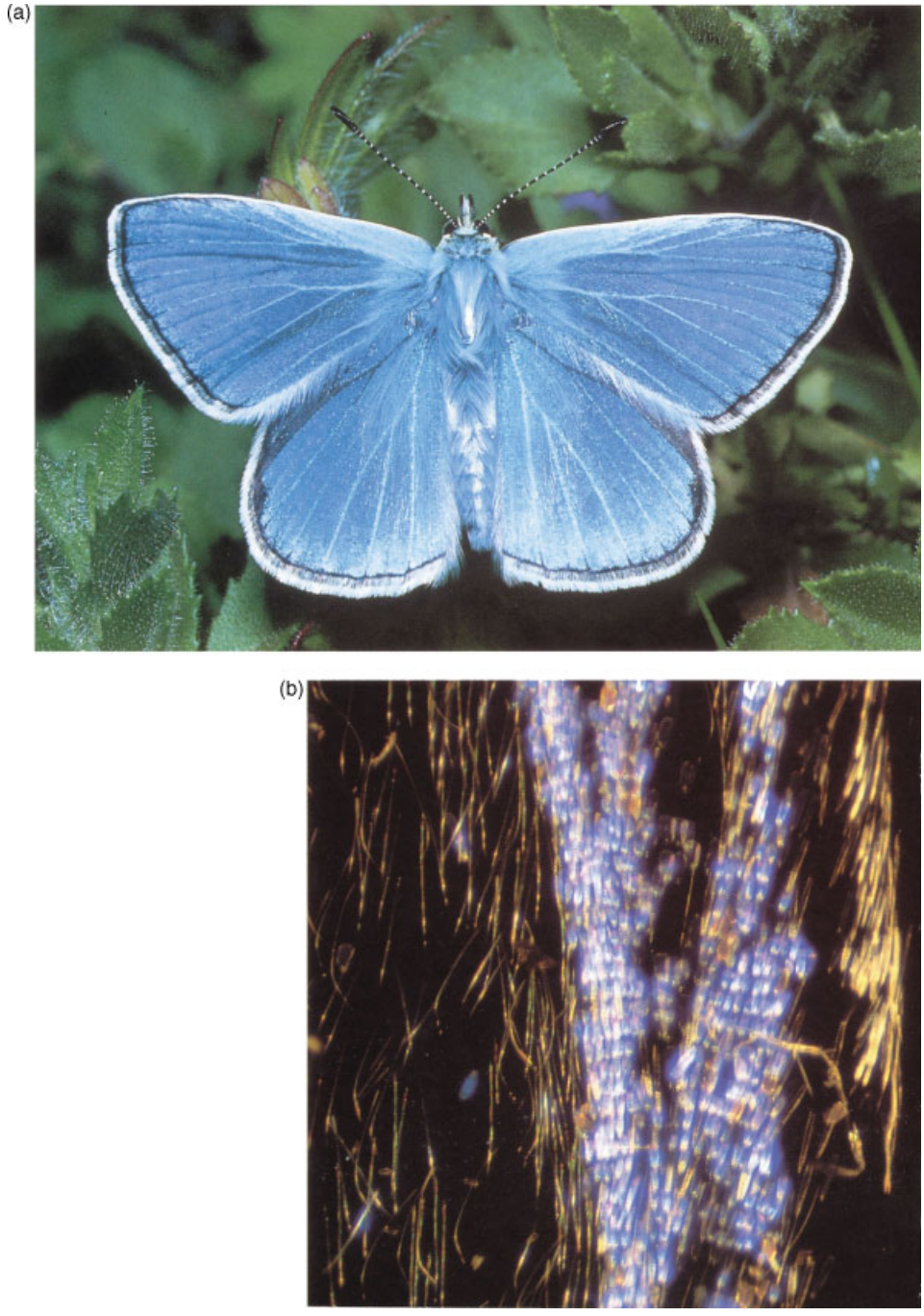

Figure 3.28 ***(a) The Common Blue butterfly* P. icarus. *(b) Scales from the wing of* P. icarus. *Only some scales have a blue reflecting microstructure. The yellow–brown scales are coloured by melanin-related pigments. [Figure (a) reproduced with kind permission of Dr J.A. Findlay]***

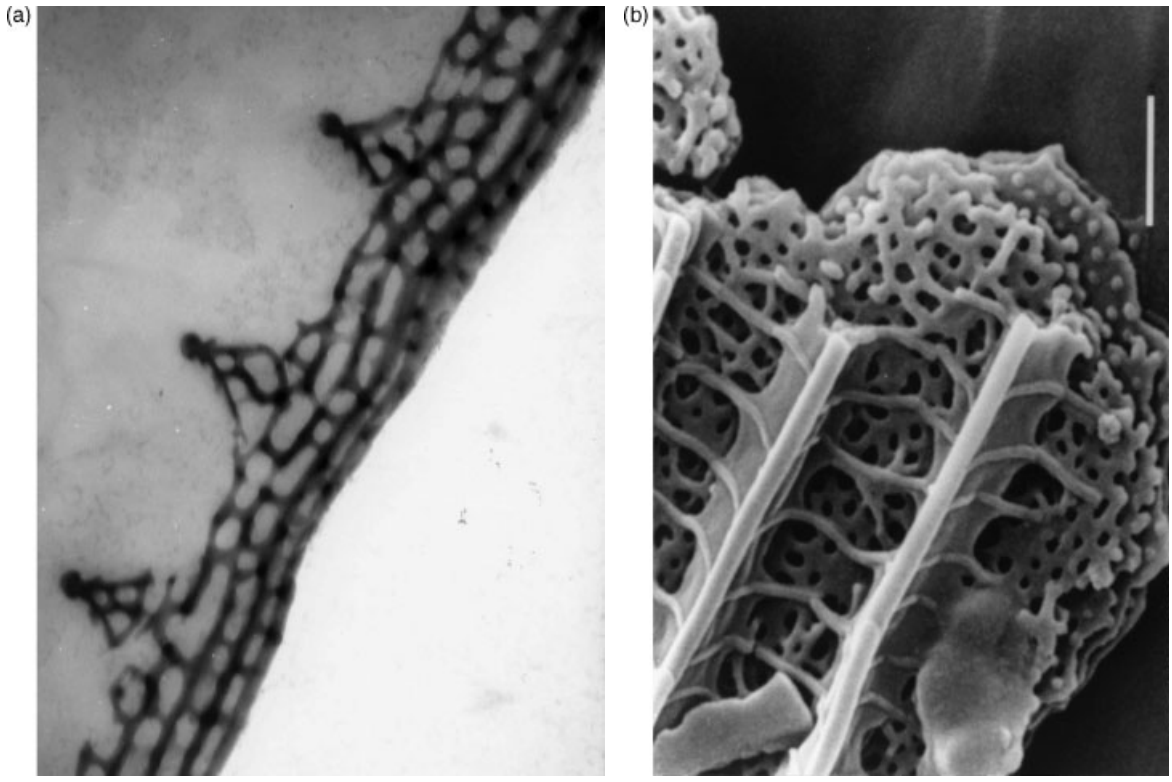

Figure 3.29 ***Electron micrographs of a blue scale from the wing of the butterfly* P. icarus. *(a) Transmission electron microscope transverse section. (b) Scanning electron micrograph of a fractured blue scale. The multiple internal layers with a perforated structure that give rise to the blue reflectivity are revealed***

It is believed that, during the formation of the parent rocks, the feldspar leading to labradorite had a homogeneous composition in which the various cations were distributed at random over the possible sites available. This is known to happen at high temperatures, and a complete solid solution is said to form between the parent phases anorthite and albite. However, at low temperatures this homogeneous solid is thermodynamically unstable and over geological time scales the sodium and calcium ions segregate to form alternating lamellae which are sodium rich and calcium rich. This also necessitates the diffusion and subsequent ordering of aluminium and silicon cations at the same time. The result is that adjacent layers possess differing refractive indices. In rare circumstances the segregation can result in lamellae which have the appropriate thickness and degree of ordering to reflect visible light and a multiple thin-film structure results. For example, an investigation of the microstructures of labradorite giving rise to a blue schiller had stacks of alternating lamellae of dimensions 72.5 nm and 65.1 nm, whereas materials showing a red schiller had lamellae of 176.6 nm alternating with lamellae of thickness 87.4 nm. As expected, the colours observed will depend upon the relative thickness of the lamellae and the angle of illumination and observation, and the refractive indices of the component lamellae. As these are subject to many variables, no two samples of labradorite from different locations are truly identical.

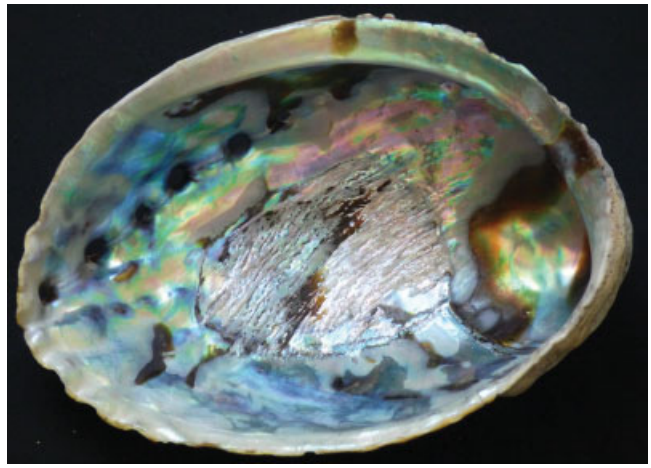

Figure 3.30 ***New Zealand paua (*H. iris*) shells showing characteristic iridescent colours that are noticeably angle dependent***

3.11.4 Mirror eyes

The design of eye most familiar to readers is the 'camera' type, which uses a lens to focus light onto a light-sensitive membrane – the retina. However, a number of different eye designs are found in nature, some of which use mirrors rather than lenses. Just one from many examples is provided by scallops of the genus *Pecten*, which

Figure 3.31 ***A specimen of labradorite from Madagascar. The colours displayed (labradoresence or schiller) change with viewing angle***

have focusing elements made up from multilayers of cytoplasm, with a refractive index of 1.34, and guanine crystals, with a refractive index of 1.83. These layers form a mirror to bring light to a focus. The total thickness of the mirror is about 6 μm and contains 60 or so layers. The multilayer mirror is hemispherical in shape and forms the interior rear surface of the eye so that rays of light entering the eye fall more or less perpendicularly upon the stack. As a rough estimate, each layer has an optical thickness of about $\lambda/4$, corresponding to strong reflection of $\lambda = 600$ nm. However, the layers of the mirror are not evenly spaced, and for this reason the eye will focus a range of wavelengths.

Appendix A3.1 The Colour of a Thin Film in White Light

Retardation[a]/nm	Colour reflected[b]	Colour transmitted[c]
	Start of first order	
0	black	bright white
40	iron grey	white
97	lavender grey	yellowish white
158	grey–blue	brownish white
218	grey	brownish yellow
234	green–white	brown
259	white	bright red
267	yellow–white	carmine red
281	straw yellow	deep violet
306	bright yellow	indigo
332	yellow	blue
430	yellow–brown	grey–blue
505	orange–red	blue–green
536	red	green
551	deep red	yellow–green
555	*End of first order; start of second order*	
565	magenta–purple	bright green
575	violet	green–yellow
589	indigo	gold
609	dark blue	yellow
664	sky blue	orange
680	blue	orange–brown
728	blue–green	brown–orange
747	green	carmine red
826	bright green	purple–red
843	yellow–green	violet–purple
866	green–yellow	violet
910	yellow	indigo
948	orange	dark blue
998	orange–red	green–blue
1050	crimson–violet	yellow–green
1100	dark violet–red	green

Appendix A3.1 (*Continued*)

Retardation[a]/nm	Colour reflected[b]	Colour transmitted[c]
1110	*End of second order; start of third order*	
1128	blue–violet	yellow–green
1151	indigo	off yellow
1258	blue–green	pink
1314	emerald green	red
1334	sea green	brown–red
1350	green	purple–violet
1376	dull green	violet
1400	yellow–green	violet–grey
1426	green–yellow	grey–blue
1450	yellow	indigo
1495	rose pink	sea green
1534	carmine red	green
1621	dull purple	dull sea green
1650	violet–grey	yellow–green
1665	*End of third order; start of fourth order*	
1682	blue–grey	green–yellow
1710	dull sea green	yellow–grey
1750	blue–green	lilac
1800	green–brown	purple–red
1811	green	carmine
1900	pale green	red
1927	greenish grey	grey–red
2000	pale grey	blue–grey
2100	carmine red	green
2220	*End of fourth order; start of fifth order*	
∼2500	green	
∼2700	pink	

Beyond this point, orders overlap and the film colour is generally pale pink or pale green in reflection.

[a] The retardation is equal to the path difference p between the interfering rays. For a single film, $p = 2nd$, where n is the refractive index of the film and d (nm) is the physical thickness. For a birefringent crystal, $p = d(|n_1 - n_2|)$, where d is the thickness of the slice of crystal and n_1 and n_2 are the effective refractive indices of the slice for light of two perpendicular polarisation directions. For a uniaxial crystal this is maximally $d(|n_0 - n_e|)$ (see Chapter 4).
[b] This colour is seen in *reflection* from a thin film in air when illuminated by white light at normal incidence. It is the same colour as that shown in *transmission* by a thin transparent plate of an anisotropic crystal viewed at normal incidence in white light *between crossed polars* (see Chapter 4).
[c] This colour is the complementary colour to that reflected and is the same as that shown in transmission by a thin film in air when illuminated by white light at normal incidence. It is the same as that shown in *transmission* by a thin transparent plate of an anisotropic crystal viewed in white light between *parallel polars* (see Chapter 4). In addition, these colours are seen in *reflection* when a thin transparent film on a substrate with a greater refractive index is viewed at normal incidence in white light.

Further Reading

Much of this chapter is concerned with thin-film optical engineering. An introduction to the topic is given by

E. Hecht, *Optics*, 4th edition, Addison-Wesley, San Francisco, 2002.
B. E. E. Saleh, M. C. Teich, *Fundamentals of Photonics*, John Wiley and Sons, Inc., New York, 1991.

An interesting historical perspective of the evolution of CDs and DVDs is
A. E. Bell, *Sci. Am*. **275** (July), 28–32 (1996).
R. L. Gunshor, A. V. Nurmikko, *Sci. Am*. **275** (July), 34–37 (1996).
G. Zorpette, *Sci. Am*. **283** (August), 19–20 (2000).
S. Nakamura, M. Riordan, *Sci. Am*. **300** (April), 54–59 (2009).

The colours produced by soap films are described and explained in
C. Isenberg, *The Science of Soap Films and Soap Bubbles*, Tieto, Clevedon (UK), 1978. Reprinted by Dover, New York, 1992.

The use of nanorods as an antireflective surface is given in
J.-Q. Xi *et al., Nat. Photonics* **1**, 176–179 (2007).

Complete coverage of the theory of single and multiple thin films is in
H. A. McLeod, *Thin-Film Optical Filters*, 3rd edition, Institute of Physics, London, 2001.

For background on the history of thin-film computation, see
O. S. Heavens, *Rev. Prog. Phys*. **23**, 1–65 (1960).

For IMOD displays, see
M. M. Waldrop, *Sci. Am*. **297** (November), 68–71 (2007).

Free versions of the software 'Filmstar', for the computation of thin-film optics (and used to compute Figure 3.20), are available from Dr F. T. Goldstein, FTG Software Associates, PO Box 597, Princeton, NJ 08542, USA (www.ftgsoftware.com).

Full information on FBGs will be found in
R. Kashyap, *Fiber Bragg Gratings*, Academic Press, London, 1999.

The topic of colour in nature is described from an evolutionary perspective, with examples of thin-film colours, mirror eyes, etc. by
A. R. Parker, *In the Blink of an Eye*, Free Press, London, 2003.

Structural colour is reviewed by
P. Vukusic, Structural color, in *Dekker Encyclopedia of Nanoscience and Nanotechnology*, J. A. Schwarz, C. I. Contescu, K. Putyera, (eds), Vol. 5, Marcel Dekker, New York, 2004, pp. 3713–3722.

Many aspects of structural colour, including butterfly scales, moth-eye AR surfaces and mirror eyes, will be found in the following papers and the references cited therein:
P. Vukusic, R. J. Wooton, J. R. Sambles, *Proc. R. Soc. Lond. Ser. B* **271**, 595–601 (2004).
P. Vukusic, J. R. Sambles, C. R. Lawrence, R. J. Wooton, *Proc. R. Soc. Lond. Ser. B* **269**, 7–14 (2002).
A. R. Parker, D. R. McKenzie, M. C. J. Large, *J. Exp. Biol*. **201**, 1307–1303 (1998).
A. R. Parker, Z. Hegedus, R. A. Watts, *Proc. Roy. Soc. Lond. Ser. B* **265**, 811–815 (1998).
A. R. Parker, *Am. Sci*. **87**, 248–255, (1999).
H. Ghiradella, *Appl. Opt*. **30**, 3492–3500 (1991).
D.-E. Nilsson, *Nature* **332**, 76–78 (1988).
A. A. Fincham, *Nature* **287**, 729–731 (1980).
M. F. Land, *Sci. Am*. **239** (December), 88–99 (1978).